In presenting this dissertation/thesis as a partial fulfillment of the requirements for an advanced degree from Emory University, I agree that the Library of the University shall make it available for inspection and circulation in accordance with its regulations governing materials of this type. I agree that permission to copy from, or to publish, this thesis/dissertation may be granted by the professor under whose direction it was written when such copying or publication is solely for scholarly purposes and does not involve potential financial gain. In the absence of the professor, the dean of the Graduate School may grant permission. It is understood that any copying from, or publication of, this thesis/dissertation which involves potential financial gain will not be allowed without written permission.

_____

Chinenye A. Idigo

Reaction Kinetics of Phenylisothiocyanate with Amino Acid Analogs

By

Chinenye A. Idigo
Master of Science

Department of Chemistry

_____
Dr. Joseph B. Justice
Adviser

_____
Dr. Vincent Conticello
Committee Member

_____
Dr. Dale E. Edmondson
Committee Member

Accepted:

_____
Lisa A. Tedesco, Ph.D.
Dean of the Graduate School

_____
Date

Reaction Kinetics of Phenylisothiocyanate with Amino Acid Analogs

By

Chinenye A. Idigo

Adviser: Joseph B. Justice, Ph.D.

An Abstract of a thesis submitted to the Faculty of the Graduate School of Emory University in partial fulfillment of the requirements for the degree of Master of Science

Department of Chemistry

2008

ABSTRACT

The kinetics of the chemical reactions of isothiocyanate derivative cocaine analogs with amino acids in the human dopamine transporter during labeling were investigated using small molecule models of the reactions. Analogs of the side-chains of cysteine, lysine and tyrosine were 1-octanethiol, phenethylamine (PEA), and phenol respectively. Phenylisothiocyanate (PITC) was used to represent isothiocyanate derivative cocaine analogs. A large excess (1mM) of each amino acid analog was reacted with PITC in an aqueous solution at pH 7.4. The experiments were repeated at pH 9.0. Pseudo first order rate constants were obtained for 1-octanethiol ($k = 1.26 \times 10^{-2}$ min^{-1} at pH 7.4 and $k = 8.73 \times 10^{-2}$ min^{-1} at pH 9.0), and PEA ($k = 2.32 \times 10^{-3}$ min^{-1} at pH 7.4 and $k = 1.51 \times 10^{-2}$ min^{-1} at pH 9.0). The results showed that 1-octanethiol was the most reactive analog at both pH 7.4 and pH 9.0. Phenol was the least reactive and showed no detectable reaction with PITC. At pH 9.0, 1-octanethiol and PEA showed a six to seven fold increase in reactivity relative to pH 7.4. The products of the reactions were confirmed using high resolution mass spectrometry. The product of the reaction of PITC and PEA was 1-phenethyl-3-phenylthiourea. The product of the reaction of PITC and 1-octanethiol was octyl phenylcarbamodithioate. 1-phenethyl-3-phenylthiourea is a stable compound and shows no detectable sign of degradation for 48 hours. Octyl phenylcarbamodithioate is much less stable and starts to show detectable degradation at 60 minutes at pH 7.4 and as early as 20 minutes at pH 9.0.

Reaction Kinetics of Phenylisothiocyanate with Amino Acid Analogs

By

Chinenye A. Idigo

Adviser: Joseph B. Justice, Ph.D.

A thesis submitted to the Faculty of the Graduate School of Emory University in partial fulfillment of the requirements for the degree of Master of Science

Department of Chemistry

2008

Table of Contents

List of Figures

Results

Discussion

List of Tables

INTRODUCTION

Background on the Human Dopamine Transporter

hDAT Function

The human dopamine transporter (hDAT) is a transmembrane protein located on the surface of presynaptic neurons. The function of hDAT is to clear dopamine from the synaptic cleft (Giros et al., 1991). Dopamine is a neurotransmitter that relays chemical signals between neurons. Dopamine is an important agent in the central nervous system, because it is involved in the perception of stimuli like pain and pleasure (Fiorino et al., 1993; Giros and Caron, 1993). The sequence of events by which dopamine release affects the postsynaptic neuron are: [Figure 1] (Giros et al., 1991)

1) Vesicles containing dopamine are released from the presynaptic neuron into the synapse.
2) Dopamine in the synapse stimulates G-protein coupled receptors on the surface of the postsynaptic neuron and causes a signal cascade.
3) hDAT takes up dopamine back into the presynaptic neuron to contribute to the end of the propagation of the signal.
4) Dopamine is either degraded or recycled for reuse in another signaling event.

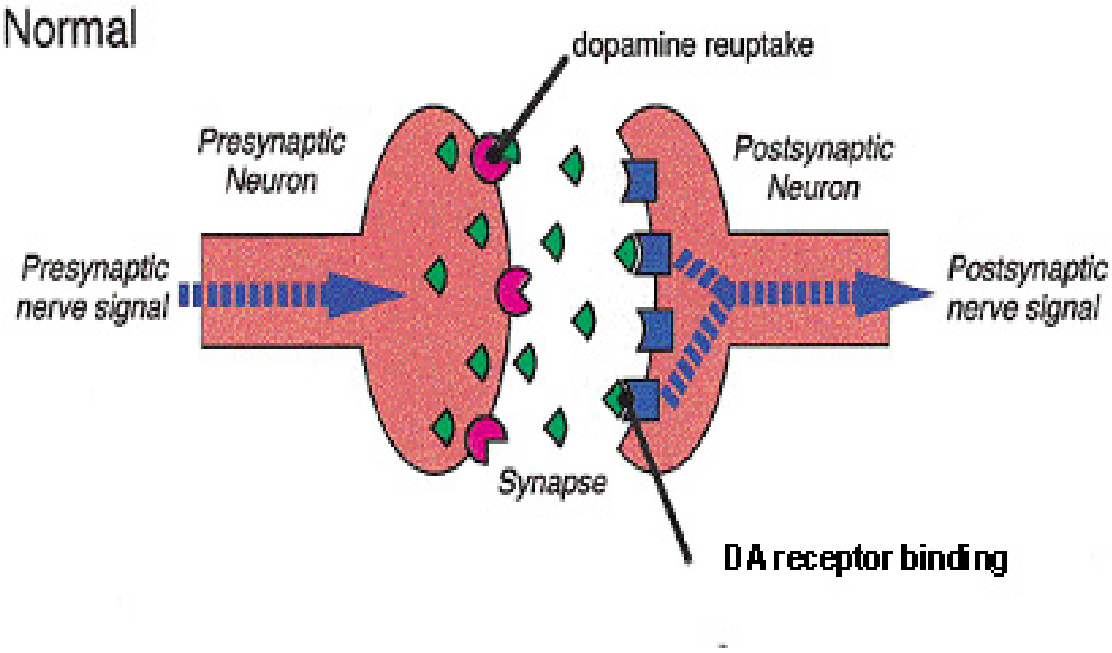

Figure 1. A schematic representation of the synapse during the transmission of a dopamine signal (Carroll and Kuhar, 1999). A nerve signal reaches the presynaptic neuron and initiates the release of dopamine into the synapse where it stimulates postsynaptic receptors.

In order to transport dopamine into the cell against its concentration gradient, hDAT is sodium and chloride-ion ($2Na^+$: Cl^-) dependent. hDAT has binding sites for both Na^+ and Cl^-, and their diffusion into the cell provides the energy to co-transport dopamine (Gu et al., 1994).

hDAT Structure and Topology

The cDNA for hDAT has been cloned (Vandenbergh et al., 1992) and the gene encodes for 620 amino acid residues. The protein has an estimated molecular weight of 80 kDa and spans the lipid bilayer of presynaptic neurons (Giros and Caron, 1993). Analysis of hDAT using hydropathy profiling indicates that the protein has twelve α-helical transmembrane domains with both the N- and C- terminus located inside the cell [Figure 2]. There is no crystal structure of hDAT available; therefore its exact three-dimensional spatial arrangement is unknown. Like most other membrane proteins, hDAT is difficult to crystallize because it denatures in the aqueous conditions necessary for crystallization (Lever et al., 2004). Other methods like solid-state NMR and mass spectrometry have not been successful in resolving the structure of hDAT either. It is difficult to use these techniques when working with hDAT because the protein has such low expression in cells and yields only small amounts of the protein.

Several indirect techniques have been employed to determine the spatial arrangement of hDAT. These techniques include site-directed mutagenesis (Kitayama et al., 1992; Wu et al., 2002), biophysical probes (Hersch et al,. 1997; Nerenberg et al., 1996; Ferrer and Javitch, 1998; Chen et al., 2000) and computational modeling (Edvardsen and Dahl, 1994; Indarte et al., 2008). hDAT labeled with target-specific monoclonal antibodies was studied by immunoperoxidase and immunogold electron microscopy and confirmed that the N terminus is located intracellularly and the second extracellular loop is located extracellularly (Hersch et al,. 1997; Nerenberg et al., 1996). Methanethiosulfonate (MTS) derivatives, which are cysteine-selective modification reagents, were used to verify that

C90 and C306 are extracellular and C135 and C342 are intracellular (Ferrer and Javitch, 1998; Chen et al., 2000). There are two cysteines located in extracellular loop 2, C180 and C189, which are thought to form a disulfide bond (Wang et al., 1995). These cysteines are conserved amongst all Na^+/Cl^- dependent transporters and their disulfide bond is believed to help hold the transporters in their functional conformation. Also located on extracellular loop 2 are three putative N-glycosylation sites (Giros and Caron, 1993).

Edvardsen and Dahl proposed a putative 3-D model of hDAT by using molecular modeling techniques to analyze hDAT's primary sequence and map it to structures of other transporters (Edvardsen and Dahl, 1994). A more recent study modeled hDAT after the template of the bacterial leucine transporter ($LeuT_{Aa}$), which is also a Na^+/Cl^- dependent transporter (Indarte et al., 2008). In 2005 $LeuT_{Aa}$ was the first Na^+/Cl^- dependent transporter crystal structure to be characterized (Yamashita et al., 2005) and it has a high sequence homology to hDAT. The Indarte et al. model of hDAT proposes a potential binding site of dopamine in a pocket where it interacts with residues in TMs 1, 3, 6, and 8.

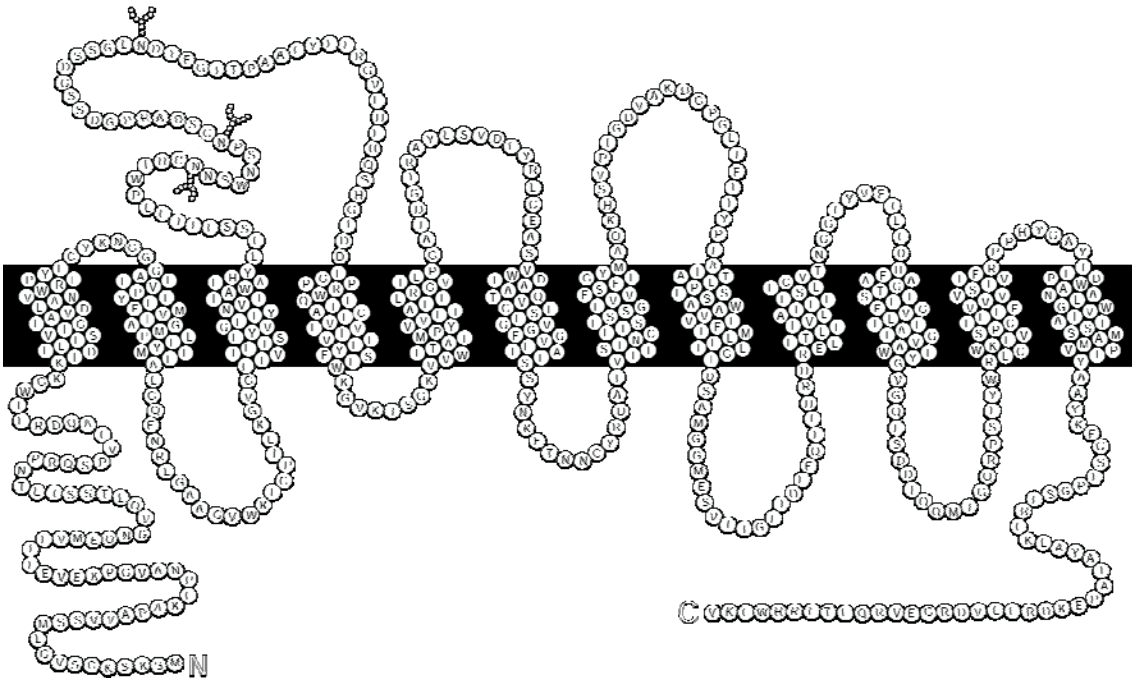

Figure 2. Sequence and topology of hDAT (Giros and Caron, 1993). There are twelve transmembrane domains with both the N- and C- terminus located intracellularly. There are three putative glycosylation sites on extracellular loop 2.

The Role of hDAT in Cocaine Addiction

Cocaine is a psychostimulant drug that can be administered intranasally, intravenously or by smoking. The principal target of cocaine is hDAT, which is why most research on cocaine therapy is aimed at the protein (Carroll et al., 1997). Cocaine disrupts dopaminergic signaling and alters the well balanced brain chemistry. Cocaine binds to hDAT and blocks the reuptake of dopamine and causes the build up of high concentrations of dopamine in the synapse. This results in an overstimulation of postsynaptic dopamine receptors and is believed to initiate euphoria and reinforcing effects (Kuhar et al., 1991). The theory that cocaine's interaction with hDAT is

responsible for its addictive nature is called the "dopamine hypothesis" (Kuhar et al., 1991). The pharmacologic goal of finding the binding site of cocaine on the human dopamine transporter is to develop a "dopamine-sparing cocaine antagonist" drug (Carroll et al., 1999; Appell et al., 2004). This presumption hinges on the hypothesis that cocaine and dopamine do not share exactly the same binding pocket on hDAT.

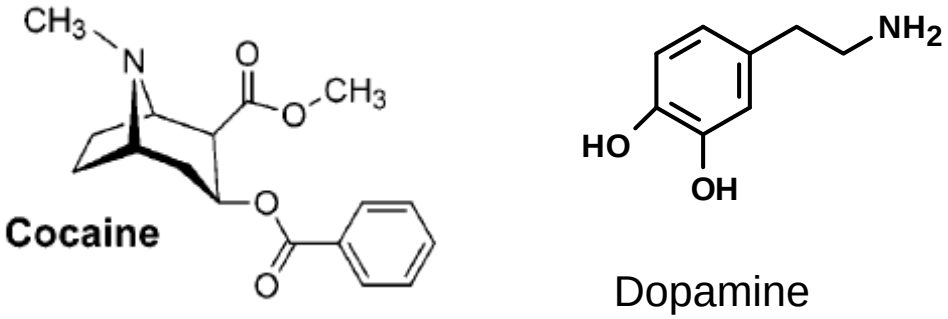

Figure 3. Chemical structures of cocaine and dopamine. Dopamine has a cathechol nucleus (two hydroxyl groups on a phenyl ring and a para R' group) with an ethylamine on it. Dopamine is the natural substrate of hDAT. Cocaine is also a substrate of hDAT.

Methods Used to Determine the Binding Site of Cocaine on hDAT

Site-Directed Mutagenesis

One of the more common methods used to investigate the binding site of cocaine on hDAT is site-directed mutagenesis. In this technique, hDAT is genetically manipulated to mutate one or more residues in the protein sequence. For example, a tryptophan residue can be replaced with a phenylalanine residue and the effect of this mutation on substrate binding and/or uptake can be analyzed. The hypothesis being that if the mutation significantly decreases cocaine binding, the residue is either directly or indirectly involved in substrate binding. The residue could be essential to substrate binding either because its absence has conformational consequences or it may be in the active site and is chemically involved in binding. A study showed that the aspartate residue D79 in TM 1 and the serine residues S356 and S359 in TM 7 are important in cocaine binding (Kitayama et al., 1992). When D79 was mutated for non-polar or positively charged residues, cocaine binding was reduced (Kitayama et al., 1992). Interestingly D79 is conserved in all monoamine transporters, but not all Na+/Cl- transporters. This led to the hypothesis that the negatively charged carboxylic acid of aspartate interacts with the positively charged amino group of cocaine (Kitayama et al., 1992). Another study showed that F105 in TM 3 is crucial in cocaine binding (Wu et al., 2002). Switching F105 to non-aromatic residues reduced cocaine binding, but switching to other aromatic residues resulted in little or no change in cocaine binding. It is hypothesized that the aromatic nature of F105 is important because it may be interacting with cocaine through pi-pi interactions. (Uhl et al., 2003)

Although site-directed mutagenesis studies have provided some leads on which residues are involved in cocaine binding, the technique has its limitations. A lot of mutations are not viable because they lead to low cell surface expression of the protein or completely non-functional hDAT. There is no way to tell for certain whether these residues identified by site-directed mutagenesis are directly involved in cocaine binding.

Photoaffinity Labeling Using Azide Derivatives

Another method used to study the binding site of cocaine on hDAT is photoaffinity labeling. In this technique, a radioactive, photoactive analog of cocaine is used to irreversibly label the protein (Vaughan et al., 2005). The photoprobe is activated by irradiation by UV light and forms a radical which will react with an amino acid in the vicinity of the binding pocket. The protein then undergoes one or more proteolytic digests and the peptide that contains the label is identified by a sequence-specific antibody. The photoaffinity labels that have been used contain an azide (-N=N) and a radioactive iodide (^{125}I) [Figure 4]. Studies using these ligands have identified what regions of DAT the amino acid they are labeling is in (Vaughan et al., 2005);

i) [^{125}I]DEEP labels TM 1

ii) [^{125}I]RTI 82 labels TMs 4-7

iii) [^{125}I]GA II 34 labels TMs 1-2

iv) [^{125}I]AD 96-129 labels both TMs 1-2 and 4-6

v) [^{125}I]MFZ 2-24 labels TMs 1-2

All the information compiled from these numerous photoaffinity labeling studies suggest that TMs 1-2 and 4-7 are spatially close to each other and the binding site of cocaine [Figure 5](Vaughan et al., 2005).

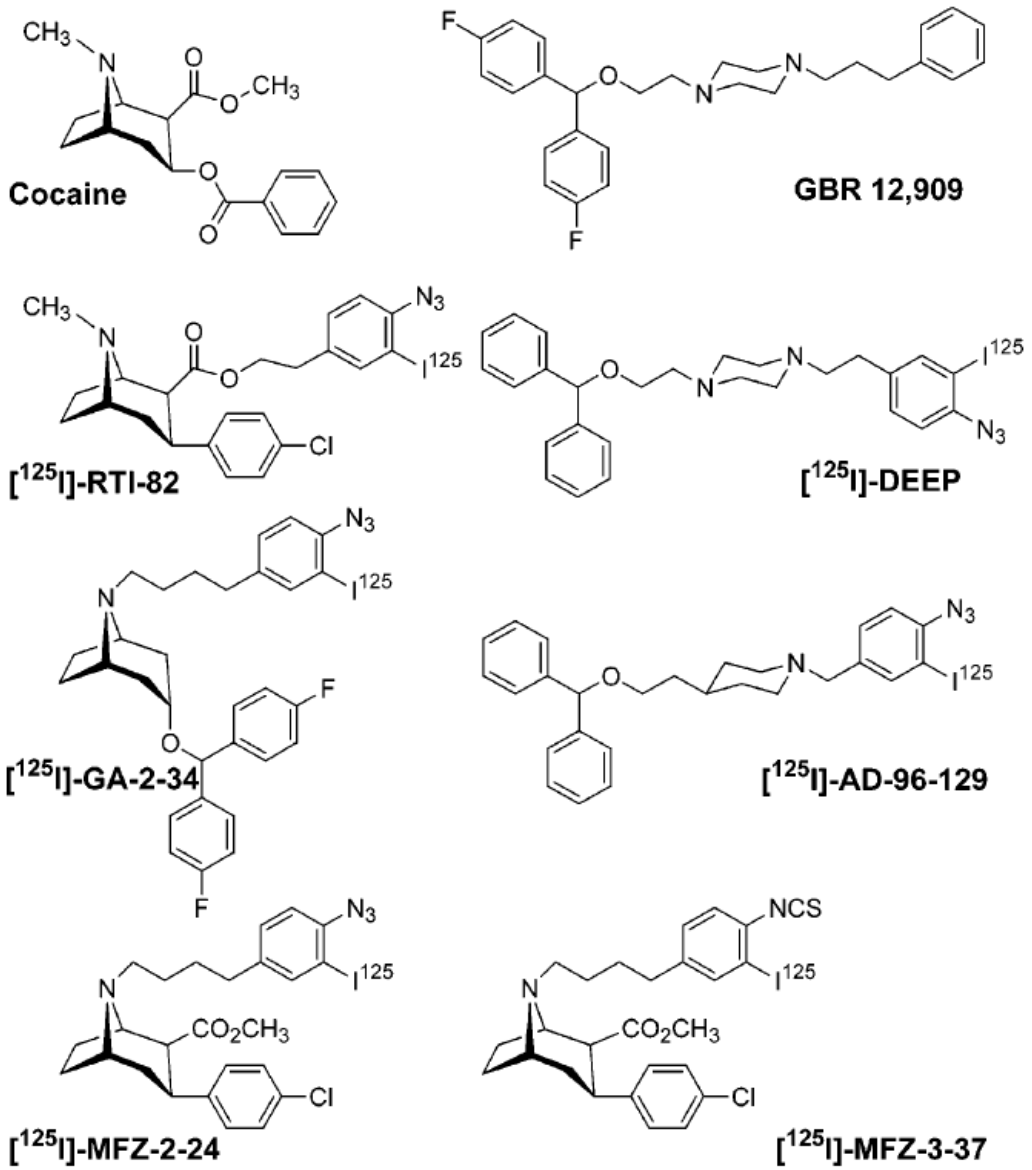

Figure 4. Chemical structures of cocaine and some cocaine analogs. [^{125}I]DEEP, [^{125}I]GA II-34, [^{125}I]AD 96-129 and [^{125}I]MFZ 2-24 contain azide groups and are used for photoaffinity labeling. [^{125}I]MFZ 3-37 contains an isothiocyanate group and is used for chemical labeling.

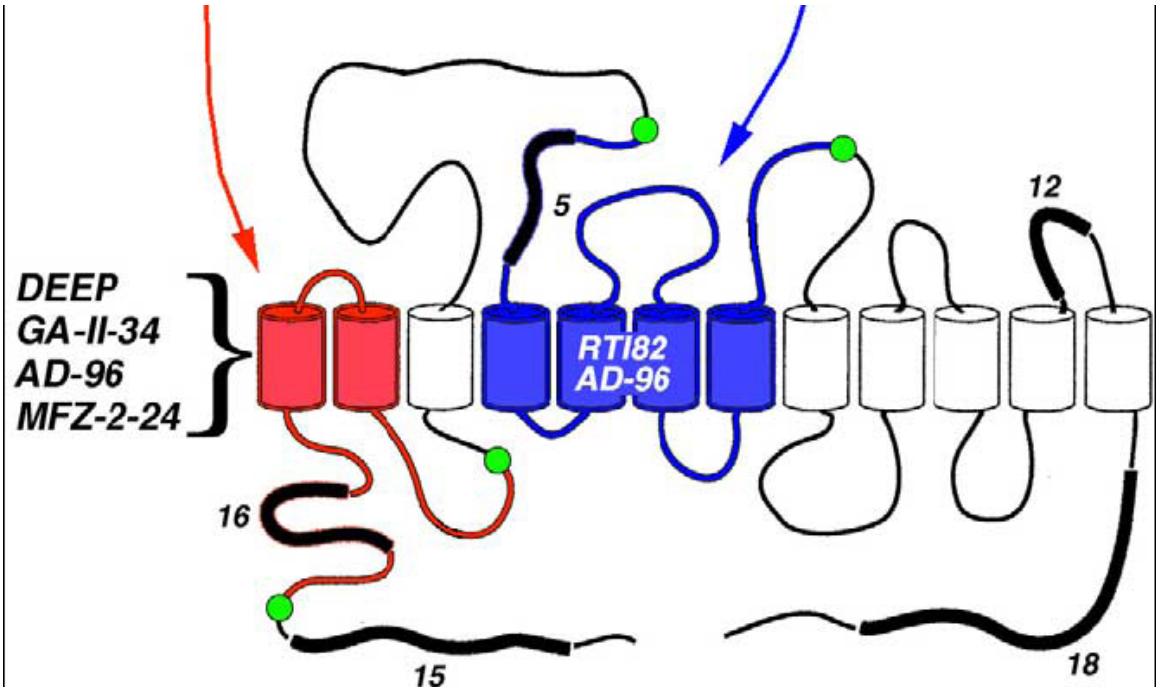

Figure 5. Schematic representation of DAT photoaffinity labeling sites (Vaughan 2005). All photoaffinity labels appear to label in the regions of TM 1-2 and/or TM 4-7.

Chemical Labeling Using Isothiocyanate Derivatives

Another class of compounds being used to label DAT contains an isothiocyanate group that chemically bonds to amino acids in the vicinity of the binding pocket. Examples of such compounds include MFZ 3-37 [Figure 4] (Zou et al., 2001) and HD 224(Murthy et al., 2007). When they were first characterized, these compounds showed promise as DAT labels because preliminary experiments indicated that they had a higher labeling efficiency that their azide photoaffinity counterparts (Lever et al., 2004). With such high labeling enough DAT would be labeled to do more extensive proteolytic digests and the smaller peptides produced could be identified by mass spectrometry. Mass spectrometry is rarely used in the analysis of cocaine analog photoaffinity labeling studies because

there is not enough labeled peptide to detect in a mass spectrometer. Antibody immunoprecipitation is usually used to identify labeled peptides, but it is limited because it is not sensitive enough to recognize very short peptide sequences. If it were possible to do more extensive digests, the labeling site of the ligand could be narrowed down to a much smaller region of DAT.

Researchers in the Justice laboratory and their colleagues have attempted labeling studies with isothiocyanate cocaine analogs, but have not yet successfully determined a binding site for these ligands. The ligands showed high affinity for the binding pocket, but when proteolytic digest were performed the label dissociated from the protein. This research thesis will attempt to understand why ligands that showed so much promise in preliminary studies, presented such difficulty in actual labeling experiments. It will investigate the kinetics of the chemical reaction between isothiocyanate and amino acids and the stability of their covalent bonds.

Project Overview and Objectives

Reactivity of Amino Acid Analogs with Phenylisothiocyanate

The experiments conducted in this research project were aimed to elucidate the kinetic properties of the chemical labeling of DAT with isothiocyanate derivative cocaine analogs. In order to do this, a small molecule model of the reaction was constructed. The amino acids studied were cysteine, lysine, and tyrosine because they are some of the amino acids with nucleophilic properties that are in the proposed ligand binding regions (Wirtz, 2004; Vaughan et al., 2005; Indarte 2008). The analogs of the side-chains of cysteine, lysine and tyrosine were 1-octanethiol, phenethylamine, and phenol respectively [Table 1]. The small molecule used to represent all isothiocyanate derivative cocaine analogs was phenylisothiocyanate (PITC) [Table 1]. The reactivity of these amino acids were compared using rate constants derived from kinetic data. The pH dependence of the rate constants was also analyzed.

Native Compound	Model Compound
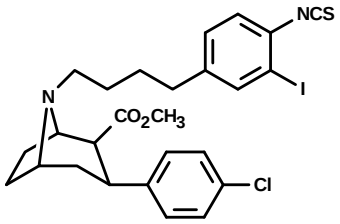 MFZ 3-37	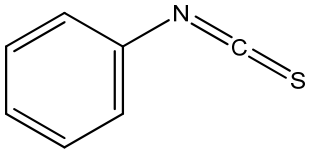 phenylisothiocyanate
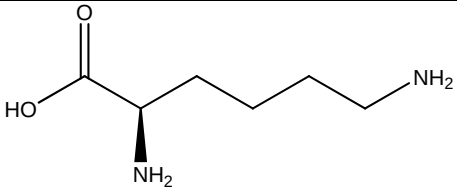 lysine	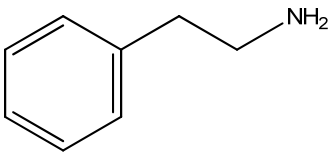 phenylethylamine
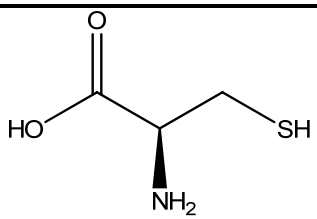 cysteine	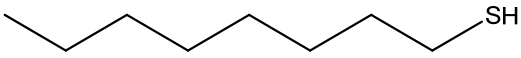 1-octanethiol
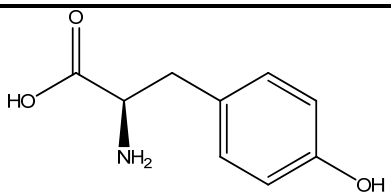 tyrosine	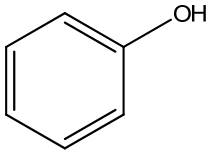 phenol

Table 1. Table of the small molecule analogs used in the experiments. The small molecule analogs of cysteine, lysine and tyrosine were 1-octanethiol, phenethylamine and phenol respectively. The small molecule analog of isothiocyanate derivative cocaine analogs like MFZ 3-37 was phenylisothiocyanate.

.

Identification of Products and Their Stability

The experiments conducted in this research project were aimed to investigate the stability of the chemical bond between isothiocyanate derivative cocaine analogs and amino acid side-chains. This information will give insight into the stability of the label during chemical labeling, protein purification, proteolytic digests and all further analysis. First the products of the reactions were identified. The product was then tested for degradation over time.

METHODS

I. Reactivity of Amino Acid Analogs

A. HPLC Analysis of the Reaction of PITC with Amino Acid Analogs at pH 7.4

Sample preparation

Stock solutions of phenylisothiocyanate (PITC), phenethylamine (PEA), 1-octanethiol, and phenol were prepared in HPLC grade acetonitrile and stored at room temperature. All reactions were also performed at room temperature. A fresh stock solution of PITC was made each week because PITC can slowly hydrolyze over time. Some reactions were performed in PBS buffer (138 mM NaCl, 2.7 mM KCl, 1.5 mM KH_2PO_4, 9.6 mM $NaH_2PO_4.H_2O$) which was prepared in distilled water and stored in a 5°C refrigerator. Concentrated NaOH and HCl were added to the buffer to achieve the desired pH.

Background Degradation of PITC at pH 7.4

Aliquots of 700 µL of PBS buffer (pH 7.4), 200 µL of acetonitrile and 100 µL of 1 mM PITC stock solution were added to a 1.5 mL Eppendorf tube. The tube was closed and vortexed and samples of this mixture were collected by syringe at times t = 0, 60, 120, 180, and 240 minutes and immediately injected into the HPLC for analysis. This procedure was repeated three times.

High Pressure Liquid Chromatography Analysis

Samples were loaded into a 20μL loop and injected into a Hewlett Packard series 1100 reverse phase HPLC. The column used was a Zorbex 5 μm C18 column with dimensions of 4.6 x 150 mm. Separation was achieved at isocratic conditions of 60 % mobile phase A (H_2O + 0.1 % Trifluoroacetic acid (TFA)), and 40% mobile phase B (acetonitrile + 0.1 % TFA). All mobile phases were filtered, and degassed before use. The flow rate through the column was 1 mL/min. A UV detector measured UV absorbance at λ = 254 nm.

Reaction of PITC and PEA at pH 7.4

Aliquots of 700 μL of PBS buffer (pH 7.4), 100 μL of acetonitrile and 100 μL of 10 mM PEA stock solution were added to a 1.5 mL Eppendorf tube. To start the reaction, 100 μL of 1 mM PITC was added and the tube was closed and vortexed. This time was recorded as the start of the reaction. Samples of this mixture were collected by syringe at times t = 1, 20, 40, 60, 100, 140, 180 and 220 minutes and immediately injected into the HPLC for analysis. Separation was achieved at isocratic conditions of 60 % mobile phase A and 40 % mobile phase B. This procedure was repeated three times.

Reaction of PITC and 1-Octanethiol at pH 7.4

Aliquots of 700 μL of PBS buffer (pH 7.4), 100 μL of acetonitrile and 100 μL of 10 mM 1-octanethiol stock solution were added to a 1.5 mL Eppendorf tube. To start the reaction, 100 μL of 1 mM PITC was added and the tube was closed and vortexed. This time was recorded as the start of the reaction. Samples of this mixture were collected by syringe at times t = 1, 20, 40, 60, 80, 100, 120, 140, 160 and 180 minutes and

immediately injected into the HPLC for analysis. Separation was achieved at isocratic conditions of 30 % mobile phase A and 70 % mobile phase B. This procedure was repeated three times.

Reaction of PITC and Phenol at pH 7.4

Aliquots of 700 µL of PBS buffer (pH 7.4), 100 µL of acetonitrile and 100 µL of 10 mM Phenol stock solution were added to a 1.5 mL Eppendorf tube. To start the reaction, 100 µL of 1 mM PITC was added and the tube was closed and vortexed. This time was recorded as the start of the reaction. Samples of this mixture were collected by syringe at times t = 1, 20, 40, 60, 100, 140, and 180 minutes and immediately injected into the HPLC for analysis. Separation was achieved at isocratic conditions of 30 % mobile phase A and 70 % mobile phase B. This procedure was repeated three times.

B. HPLC Analysis of the Reaction of PITC with Amino Acid Analogs at pH 9.0

Background Degradation of PITC at pH 9.0

The above procedure "*Background Degradation of PITC at pH 7.4"* was repeated but the PBS buffer was at pH 9.0. Samples were injected into the HPLC at t= 0, 30, 60, 90, 120, and 150 minutes. This procedure was repeated three times.

Reaction of PITC and PEA at pH 9.0

The above procedure "*Reaction of PITC and PEA at pH 7.4"* was repeated but the PBS buffer was at pH 9.0. Samples were injected into the HPLC at t= 1, 20, 40, 60, 80, 100, and 120 minutes. This procedure was repeated three times.

Reaction of PITC and 1-Octanethiol at pH 9.0

The above procedure "*Reaction of PITC and 1-Octanethiol at pH 7.4"* was repeated but the PBS buffer was at pH 9.0. Samples were injected into the HPLC at t= 1, 20, 40, 60, and 80 minutes. This procedure was repeated three times.

Reaction of PITC and Phenol at pH 9.0

The above procedure "*Reaction of PITC and Phenol at pH 7.4"* was repeated but the PBS buffer was at pH 9.0. Samples were injected into the HPLC at t= 1, 20, 40, 60, 80, and 100 minutes. This procedure was repeated three times.

II. Identification of Products and Their Stability

A. Identification of Products

Collection of the Product of the Reaction of PITC and PEA

Aliquots of 700 µL of PBS buffer (pH 7.4), 100 µL of acetonitrile and 100 µL of 1 M PEA stock solution were added to a 1.5 mL Eppendorf tube. To start the reaction, 100 µL of 1 M PITC was added and the tube was closed and vortexed. The reaction was allowed to sit for 3 hours. At this time, a 20 µL sample was injected into the HPLC. A fraction

was collected of the product as it came out of the column. The fraction was collected at the retention time that corresponded to the product peak. This fraction was then submitted to the high resolution mass spectrometry laboratory.

High Resolution Mass Spectrometry Analysis

The submitted samples were run on an FT-ICR LTQ-FT high resolution mass spectrometer by Uliana Danilienko.

Collection of the Product of the Reaction of PITC and 1-Octanethiol

Aliquots of 700 µL of PBS buffer (pH 7.4), 100 µL of acetonitrile and 100 µL of 1 M 1-octanethiol stock solution were added to a 1.5 mL Eppendorf tube. To start the reaction, 100 µL of 1 M PITC was added and the tube was closed and vortexed. The reaction was allowed to sit for 3 hours. At this time, a 20 µL sample was injected into the HPLC. A fraction was collected of the product as it came out of the column. The fraction was collected at the retention time that corresponded to the product peak. This fraction was then submitted to the high resolution mass spectrometry laboratory.

B. Stability of Products

Stability of the Product of the Reaction of PITC and PEA at pH 7.4

The above procedure "*Reaction of PITC and PEA at pH 7.4"* was repeated but samples were injected into the HPLC at t= 3, 6, 18, 30, 54 hours. This procedure was repeated three times.

Stability of the Product of the Reaction of PITC and PEA at pH 9.0

The above procedure "*Reaction of PITC and PEA at pH 9.0"* was repeated but samples were injected into the HPLC at t= 3, 6, 18, 30 and 54 hours. This procedure was repeated three times.

Stability of the Product of the Reaction of PITC and 1-Octanethiol at pH 7.4

The above procedure "*Reaction of PITC and 1-Octanethol at pH 7.4"* was repeated but samples were injected into the HPLC at t= 60, 80, 100, 120, 140, 160, 180 minutes. This procedure was repeated three times.

Stability of the Product of the Reaction of PITC and 1-Octanethiol at pH 9.0

The above procedure "*Reaction of PITC and 1-Octanethiol at pH 9.0"* was repeated but samples were injected into the HPLC at t= 20, 40, 60 and 80 minutes. This procedure was repeated three times.

DATA ANALYSIS

All the data collected from the experiments detailed in the Methods section were graphed and analyzed in ORIGIN 6.1 software. A statistical evaluation was performed on the data to obtain mean and error values. The error values used were the standard deviations of the data from the mean. For each trial, a graph was made of these mean values and their error bars. The data were then fit to a function of the form:

$$y = y_0 * e^{(-kt)}$$

where: y = relative peak height in %
y_0 = initial relative peak height in %
k = rate constant in min^{-1}
t = time in minutes

The purpose of fitting the data to this equation was to get values for the first order rate constant, k. The data collected were fit to this equation because the reactions were pseudo first order. A pseudo first order reaction is one where the rate of reaction should depend on the concentration of two reagents but because one of the reagents is in so much excess and therefore constant, the rate of the reaction is dependent on only the other reagent. In these series of reactions the amino acid analogs were in ten times excess of PITC and this constitutes as a pseudo first order reaction.

EXPERIMENTAL DATA

I.A. HPLC Analysis of the Reaction of PITC with Amino Acid Analogs

HPLC Data of the Degradation of PITC at pH 7.4

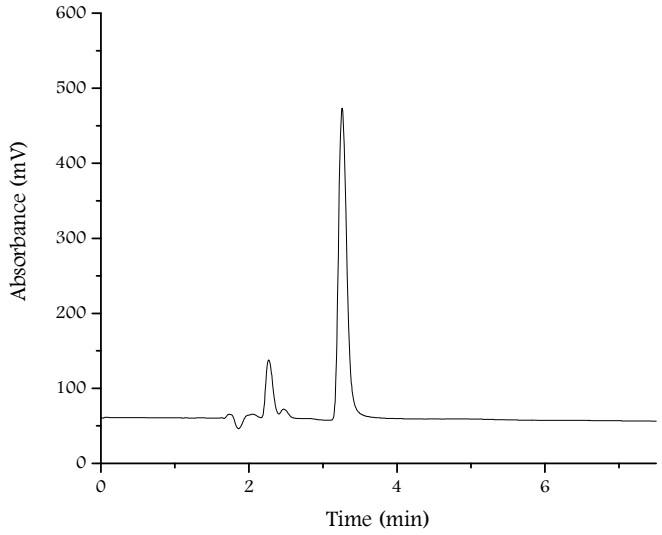

Figure 6. HPLC Chromatogram of 0.1 mM PITC solvated in 70% PBS Buffer (pH 7.4) / 30% acetonitrile at time point t = 0 minutes. The mobile phase used to achieve this separation was 70% acetonitrile (0.1% TFA) / 30% H_20 (0.1% TFA). The retention time for PITC is between 3.3 minutes

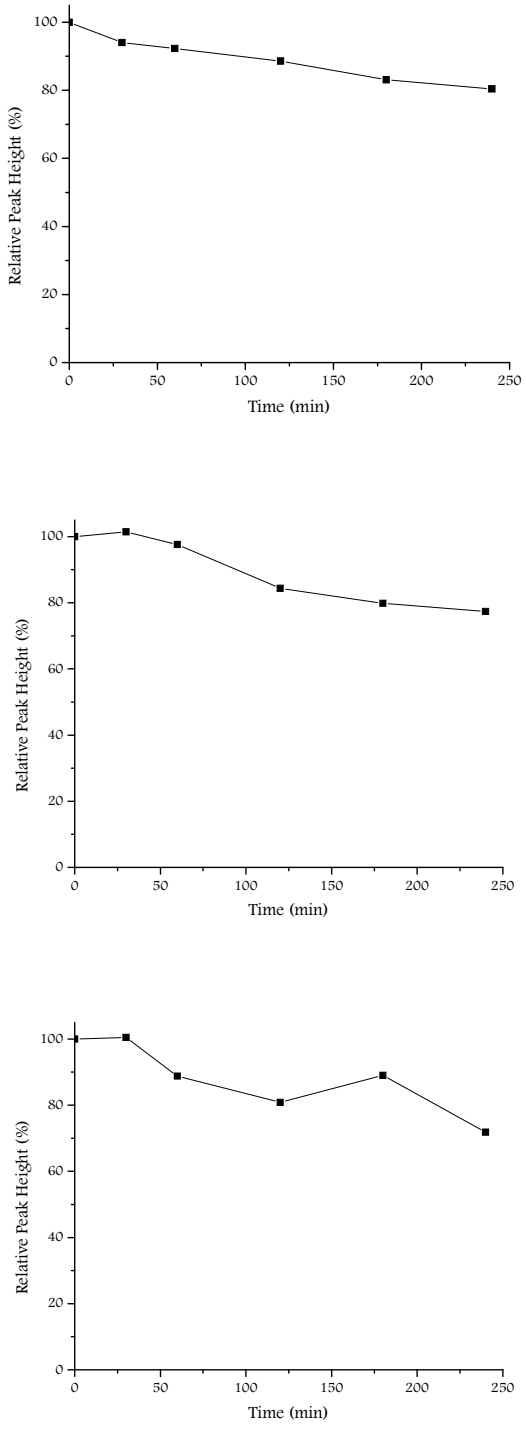

Figure 7. Three sets of data showing the time course of the degradation of 0.1 mM PITC solvated in 70% PBS buffer (pH 7.4) / 30% acetonitrile.

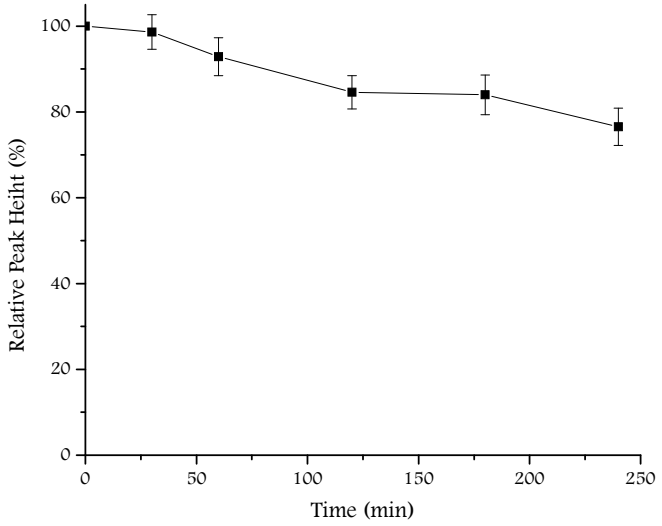

Figure 8. Time course (n=3) of the degradation of 0.1 mM PITC solvated in 70% PBS buffer (pH 7.4) / 30% acetonitrile. The error bars represent the standard deviation of data from the mean

HPLC Data of the Reaction of PITC and PEA at pH 7.4

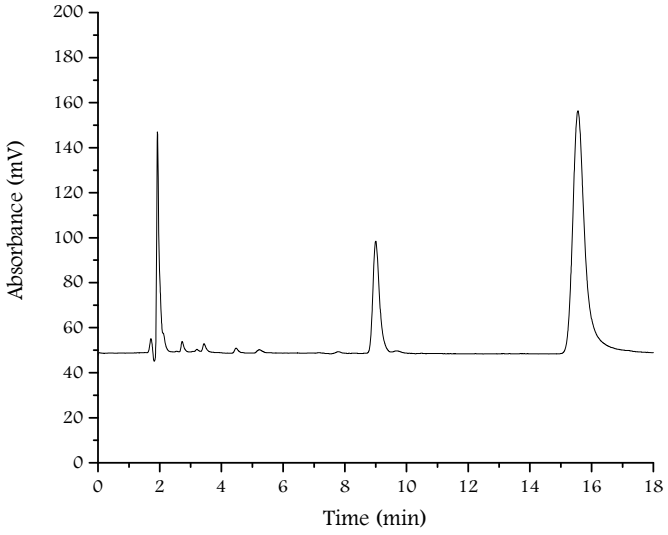

Figure 9. HPLC Chromatogram of a sample collected from the reaction of 0.1 mM PITC and 1 mM PEA solvated in 70% PBS Buffer (pH 7.4) / 30% acetonitrile at time point t = 40 minutes. The mobile phase used to achieve this separation was 40% acetonitrile (0.1% TFA) / 60% H_20 (0.1% TFA). The retention time for PITC is 15.9 minutes. The retention time of PEA is 2.0 minutes. The retention time of the product of the reaction is 9.0 minutes.

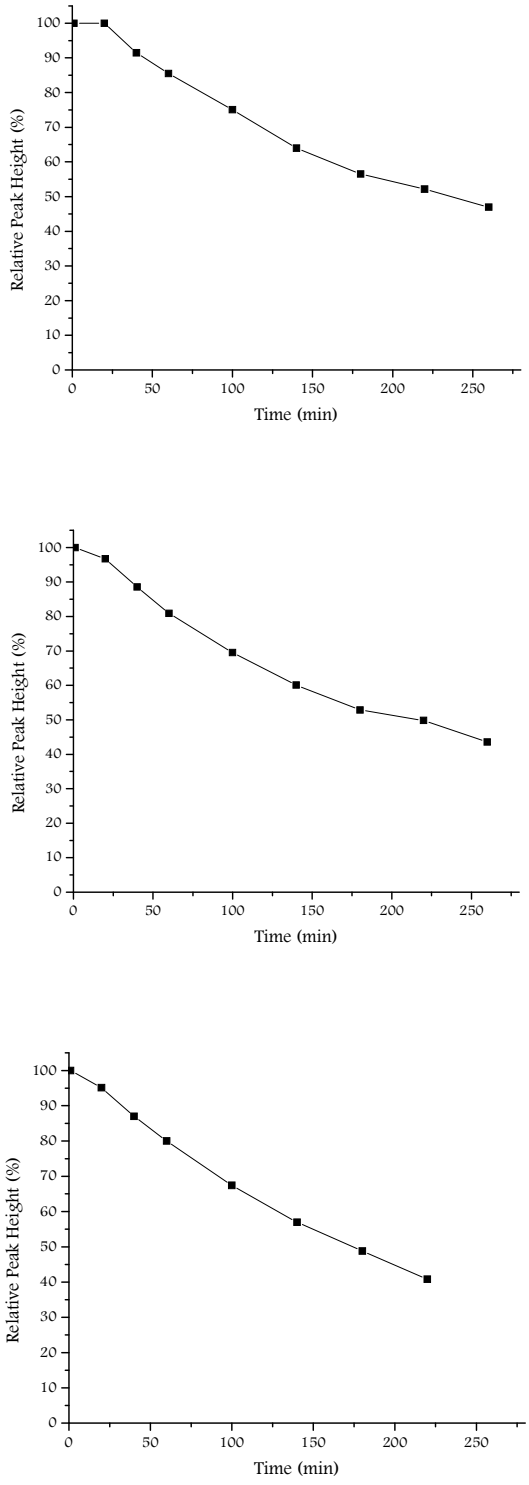

Figure 10. Three data sets showing the time course of the reaction of 0.1 mM PITC and 1 mM PEA solvated in 70% PBS buffer (pH 7.4) / 30% acetonitrile.

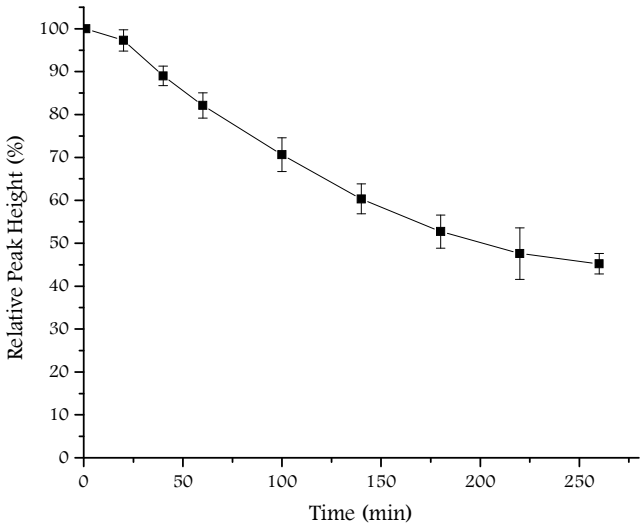

Figure 11. Time course (n =3) of the reaction of 0.1 mM PITC and 1 mM PEA solvated in 70% PBS buffer (pH 7.4) / 30% acetonitrile. The error bars represent the standard deviation of data from the mean

HPLC Data of the Reaction of PITC and 1-Octanethiol at pH 7.4

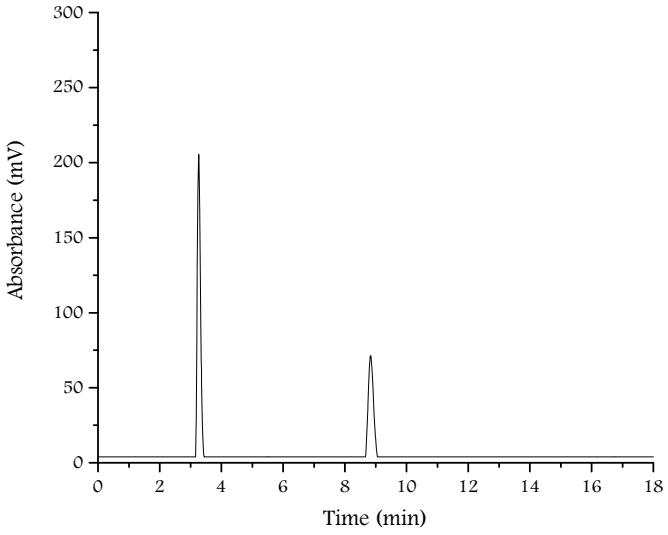

Figure 12. HPLC Chromatogram of a sample collected from the reaction of 0.1 mM PITC and 1 mM 1-octanethiol solvated in 70% PBS Buffer (pH 7.4) / 30% acetonitrile at time point t = 60 minutes. The mobile phase used to achieve this separation was 70% acetonitrile (0.1% TFA) / 30% H_20 (0.1% TFA). The retention time of PITC is 3.3 minutes. The retention time of the product of the reaction is 8.8 minutes.

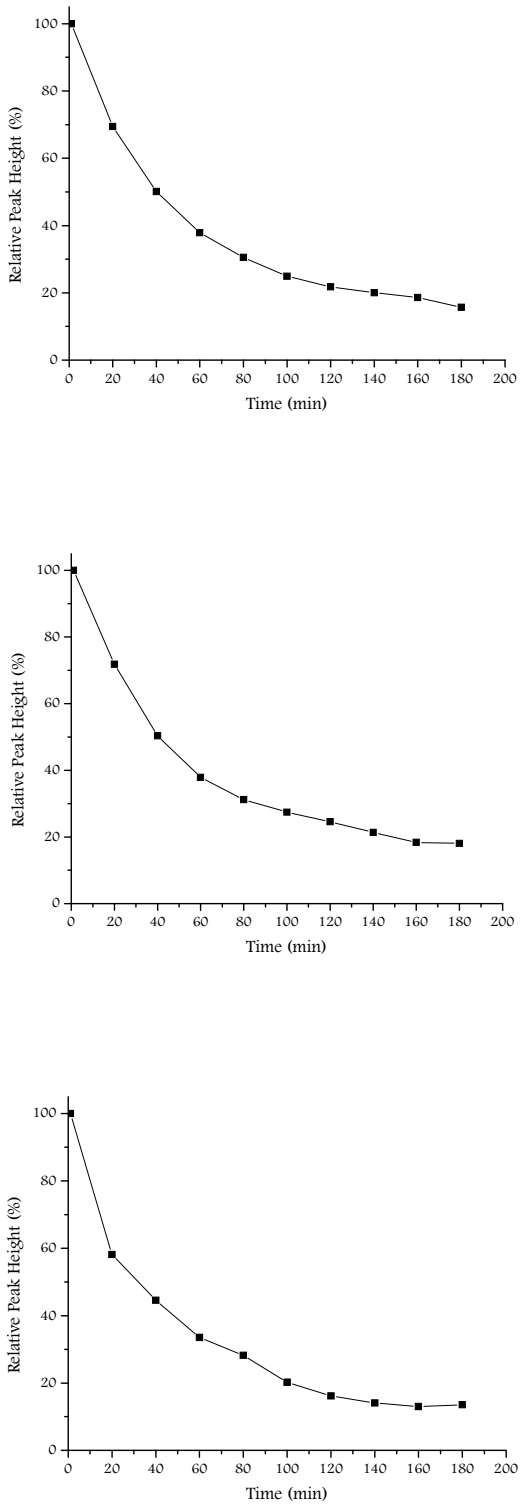

Figure 13. Three data sets of the time course of the Reaction of 0.1 mM PITC and 1 mM 1-octanethiol solvated in 70% PBS buffer (pH 7.4) / 30% acetonitrile.

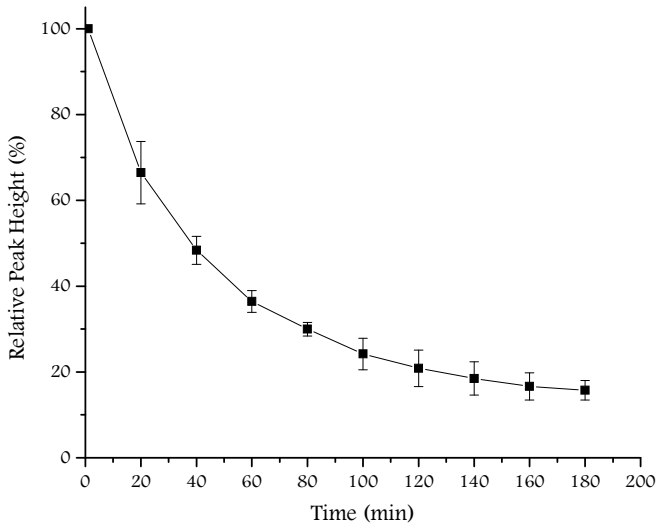

Figure 14. Time course (n=3) of the reaction of 0.1 mM PITC and 1 mM 1-octanethiol solvated in 70% PBS buffer (pH 7.4) / 30% acetonitrile. The error bars represent the standard deviation of data from the mean.

HPLC Data of the Reaction of PITC and Phenol at pH 7.4

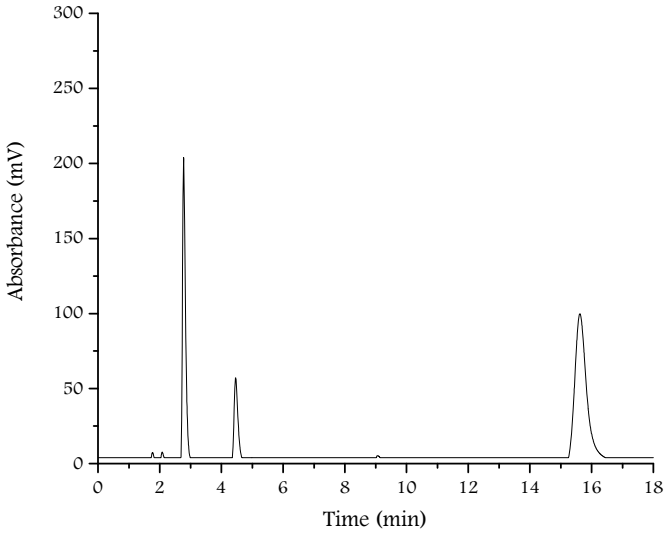

Figure 15. HPLC Chromatogram of a sample collected from the reaction of 0.1 mM PITC and 1 mM phenol solvated in 70% PBS Buffer (pH 7.4) / 30% acetonitrile at time point t = 100 minutes. The mobile phase used to achieve this separation was 40% acetonitrile (0.1% TFA) / 60% H_20 (0.1% TFA). The retention time for PITC is 15.8 minutes. The retention time of phenol is 2.7 minutes.

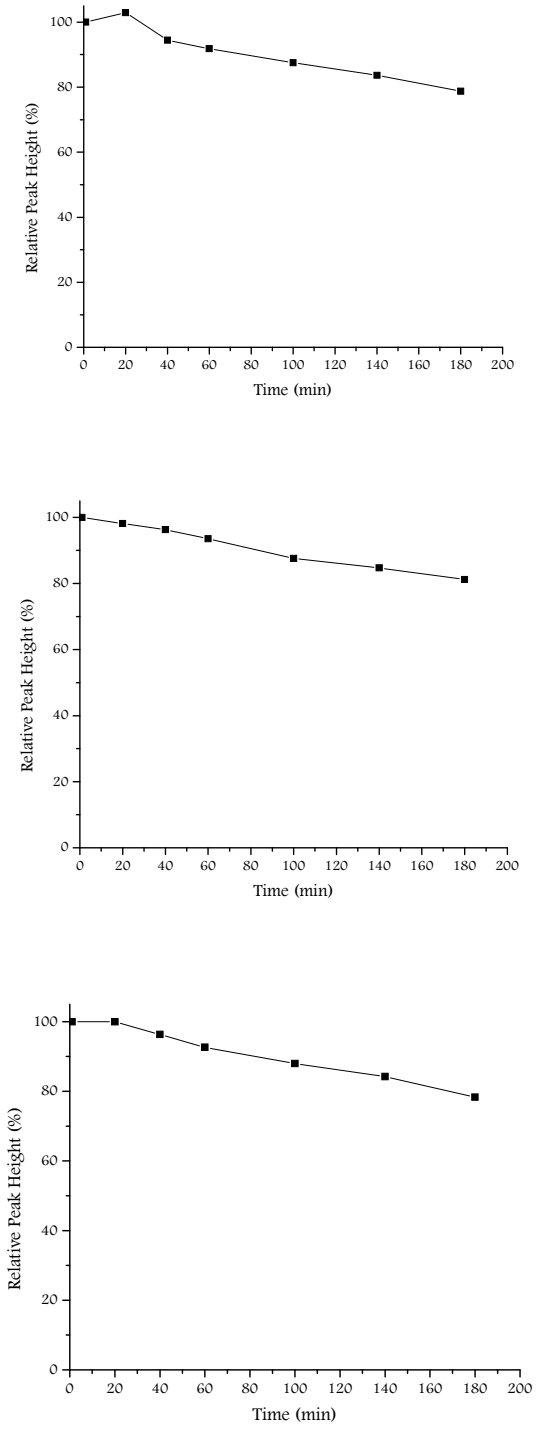

Figure 16. Three data sets of the time course of the reaction of 0.1 mM PITC and 1 mM phenol solvated in 70% PBS buffer (pH 7.4) / 30% acetonitrile.

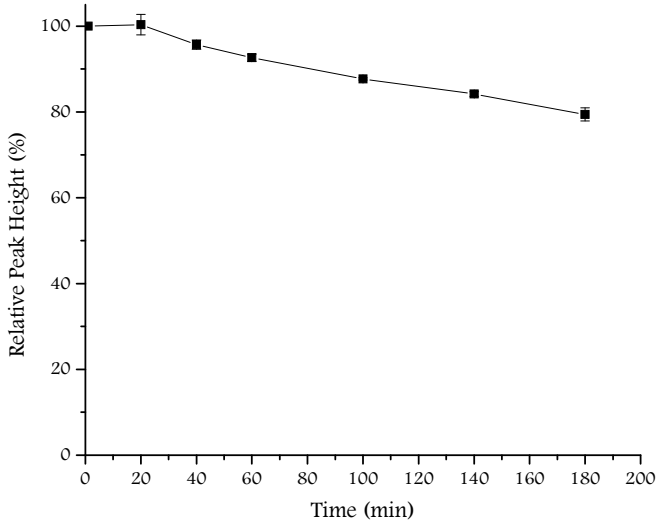

Figure 17. Time course (n=3) of the reaction of 0.1 mM PITC and 1 mM phenol solvated in 70% PBS buffer (pH 7.4) / 30% acetonitrile. The error bars represent the standard deviation of data from the mean

HPLC Data of the Degradation of PITC at pH 9.0

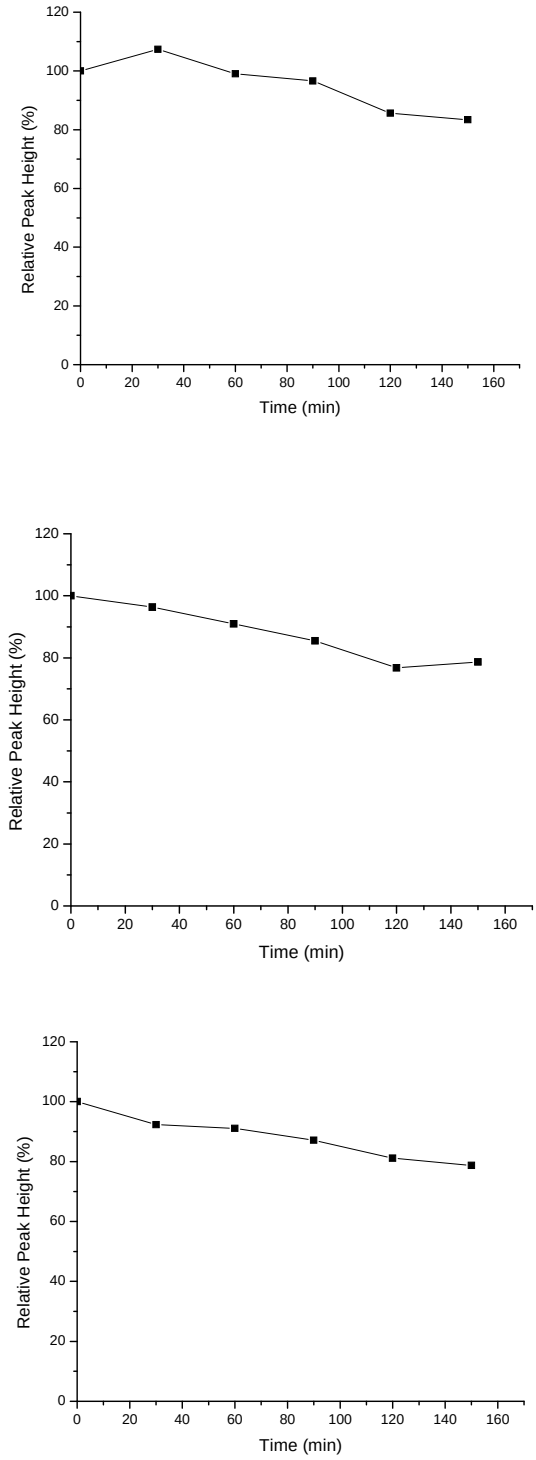

Figure 18. Three data sets of the time course of the degradation of 0.1 mM PITC solvated in 70% PBS buffer (pH 9.0) / 30% acetonitrile.

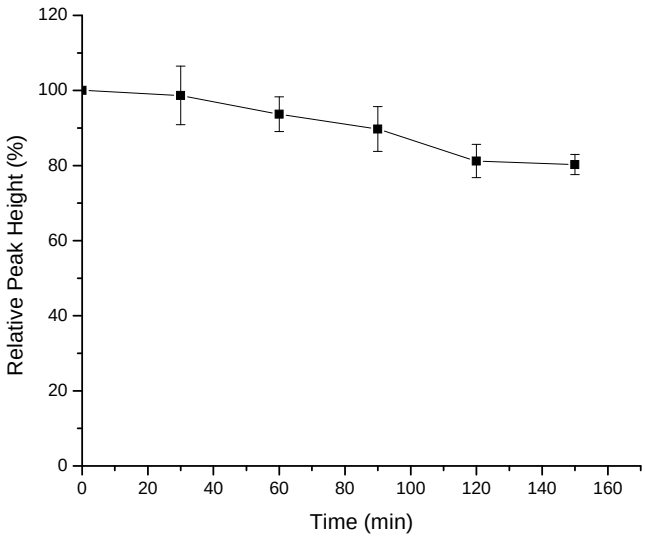

Figure 19. Time course (n=3) of the degradation of 0.1 mM PITC solvated in 70% PBS buffer (pH 9.0) / 30% acetonitrile. The error bars represent the standard deviation of data from the mean

HPLC Data of the Reaction of PITC and PEA at pH 9.0

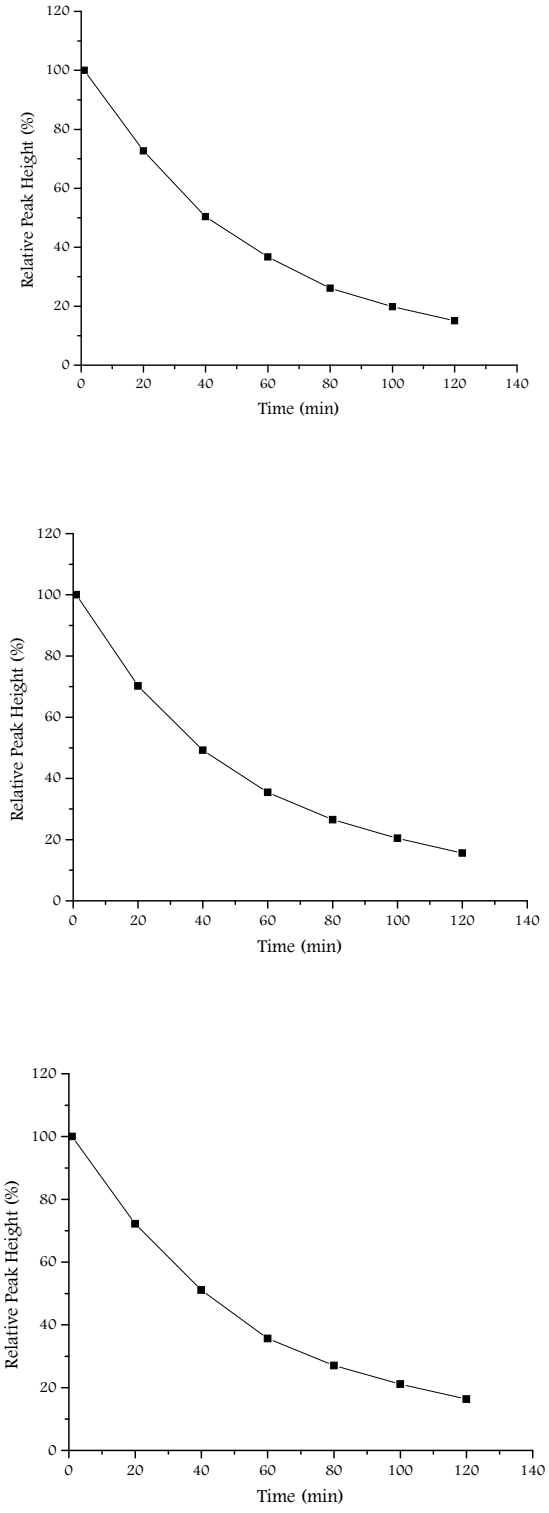

Figure 20. Three data sets of the time course (n=3) of the reaction of 0.1 mM PITC and 1 mM PEA solvated in 70% PBS buffer (pH 9.0) / 30% acetonitrile.

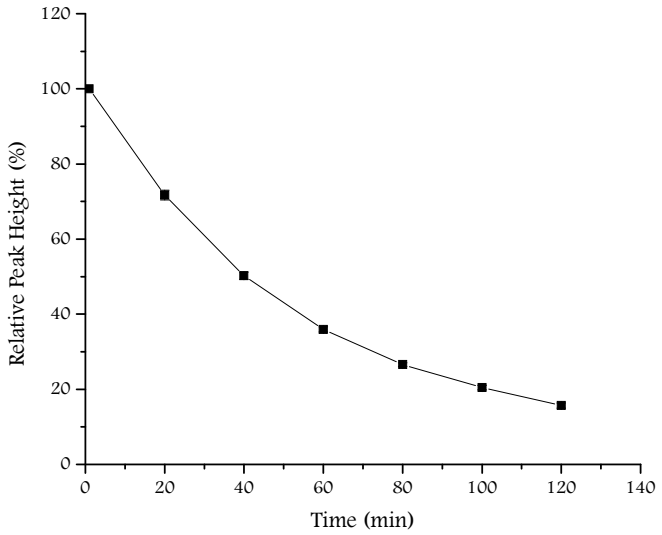

Figure 21. Time course (n=3) of the reaction of 0.1 mM PITC and 1 mM PEA solvated in 70% PBS buffer (pH 9.0) / 30% acetonitrile. The error bars represent the standard deviation of data from the mean

HPLC Data of the Reaction of PITC and 1-Octanethiol at pH 9.0

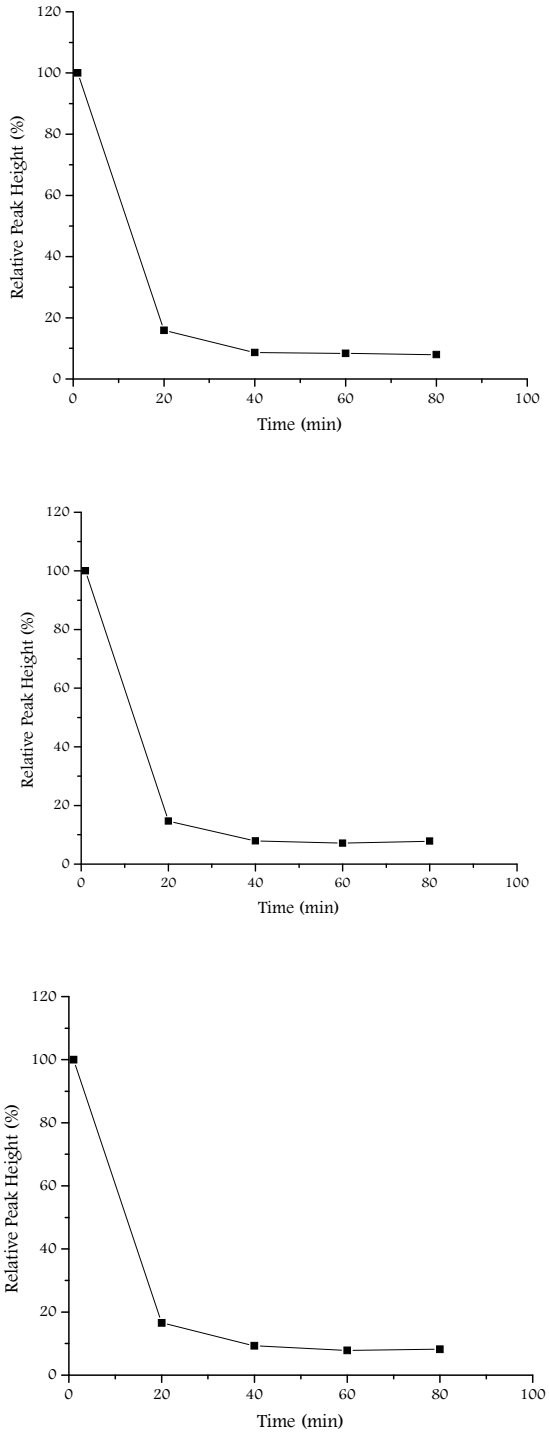

Figure 22. Three data sets of the time course (n=3) of the reaction of 0.1 mM PITC and 1 mM 1-octanethiol solvated in 70% PBS buffer (pH 9.0) / 30% acetonitrile.

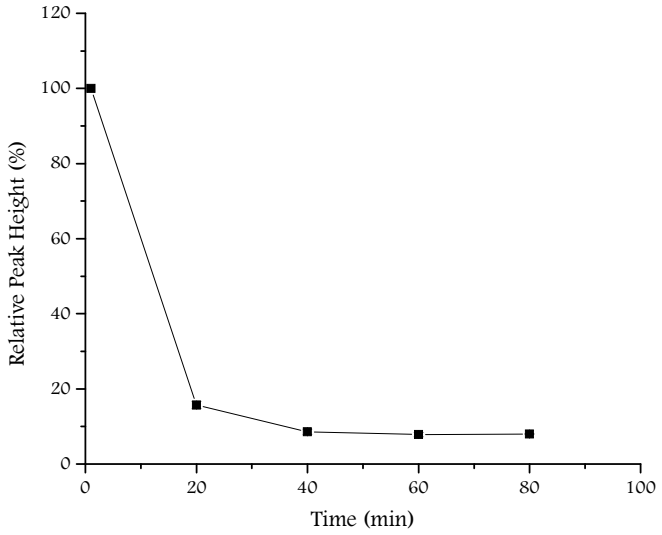

Figure 23. Time course (n=3) of the reaction of 0.1 mM PITC and 1 mM 1-octanethiol solvated in 70% PBS buffer (pH 9.0) / 30% acetonitrile. The error bars represent the standard deviation of data from the mean

HPLC Data of the Reaction of PITC and Phenol at pH 9.0

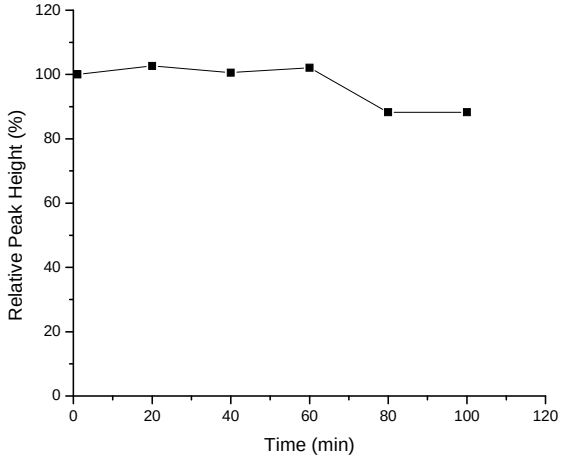

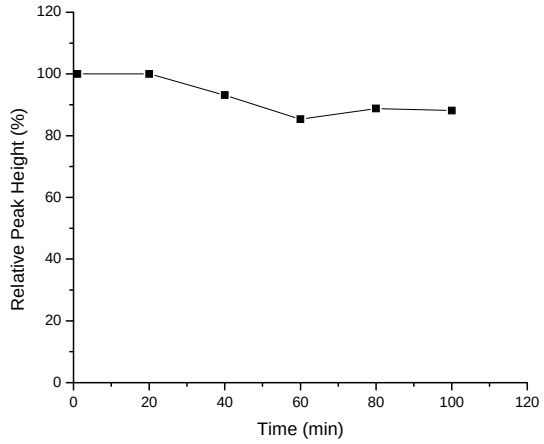

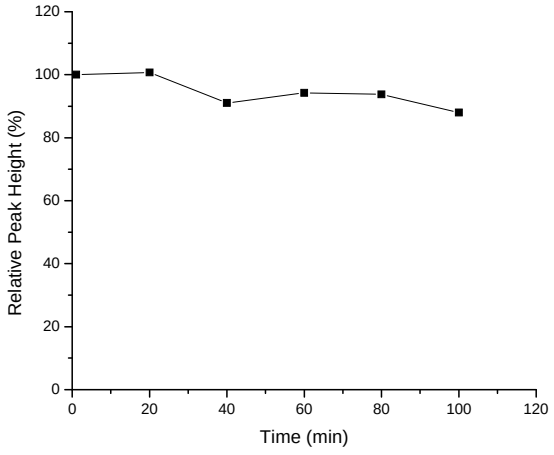

Figure 24. Three data sets of the time course (n=3) of the reaction of 0.1 mM PITC and 1 mM phenol solvated in 70% PBS buffer (pH 9.0) / 30% acetonitrile.

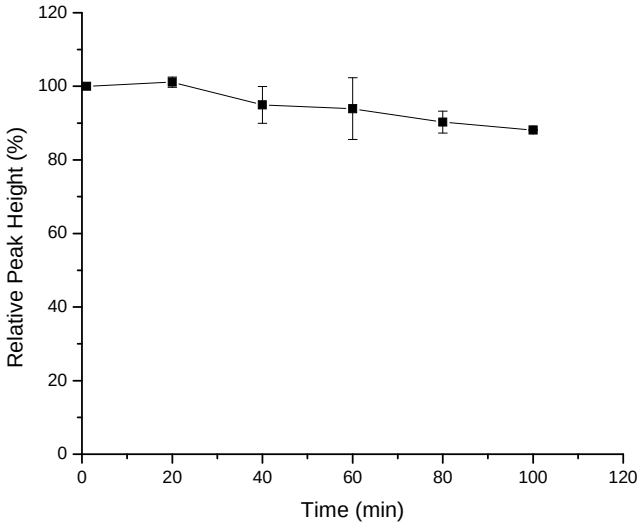

Figure 25. Time course (n=3) of the reaction of 0.1 mM PITC and 1 mM phenol solvated in 70% PBS buffer (pH 9.0) / 30% acetonitrile. The error bars represent the standard deviation of data from the mean.

II.A. High Resolution Mass Spectrometry Analysis of Products

Mass Spectrometry Analysis of the Product of the Reaction of PITC and PEA

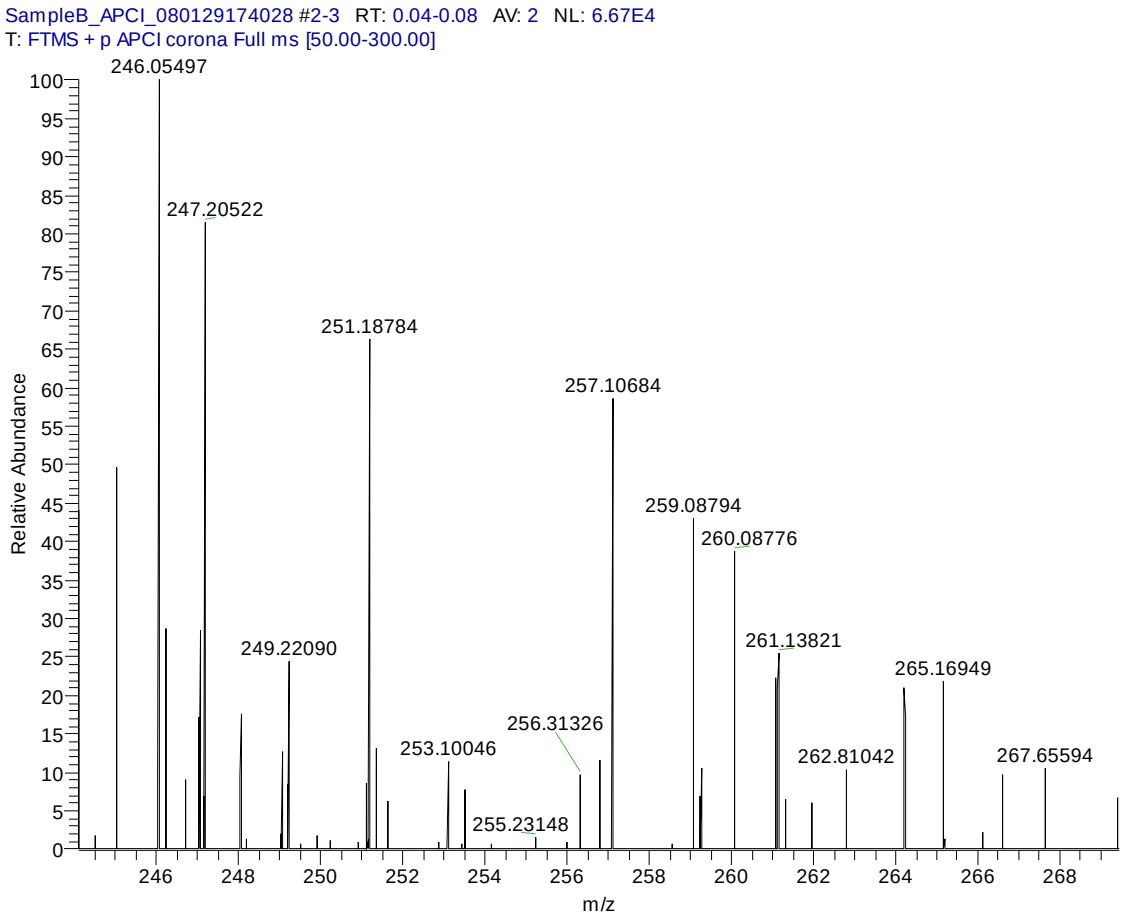

Figure 26. Mass spectrum of the product of the reaction of PITC and PEA. The sample was successfully ionized using atmospheric pressure chemical ionization (APCI) technique. The peak of interest has a mass to charge ratio of 257.10684

Elemental composition search on mass 257.10684

m/z= 252.10684-262.10684

m/z	Theo. Mass	Delta (mmu)	RDB equiv.	Composition
257.10684	257.10667	0.17	4.5	$C_{10}H_{17}O_2N_4{}^{32}S_1$
	257.10649	0.35	1.5	$C_2H_{13}O_5N_{10}$
	257.10733	-0.49	13.5	$C_{18}H_{13}N_2$
	257.10783	-0.99	1.0	$C_4H_{15}O_6N_7$
	257.10802	-1.18	4.0	$C_{12}H_{19}O_3N_1{}^{32}S_1$
	257.10534	1.50	-0.5	$C_9H_{21}O_6{}^{32}S_1$
	257.10533	1.51	5.0	$C_8H_{15}O_1N_7{}^{32}S_1$
	257.10465	2.19	9.0	$C_{15}H_{15}O_3N_1$
	257.10918	-2.34	0.5	$C_6H_{17}O_7N_4$
	257.10399	2.85	0.0	$C_7H_{19}O_5N_3{}^{32}S_1$
	257.10399	2.85	5.5	$C_6H_{13}N_{10}{}^{32}S_1$
	257.10330	3.54	9.5	$C_{13}H_{13}O_2N_4$
	257.11051	-3.67	5.5	$C_7H_{13}O_3N_8$
	257.11052	-3.68	0.0	$C_8H_{19}O_8N_1$
	257.11070	-3.86	8.5	$C_{15}H_{17}N_2{}^{32}S_1$
	257.10265	4.19	0.5	$C_5H_{17}O_4N_6{}^{32}S_1$
	257.10197	4.87	4.5	$C_{12}H_{17}O_6$
	257.10196	4.88	10.0	$C_{11}H_{11}O_1N_7$

Figure 27. Elemental analysis of the peak of interest which has a mass to charge ratio of 257.10684.

Mass Spectrometry Analysis of the Product of the Reaction of PITC and 1-Octanethiol

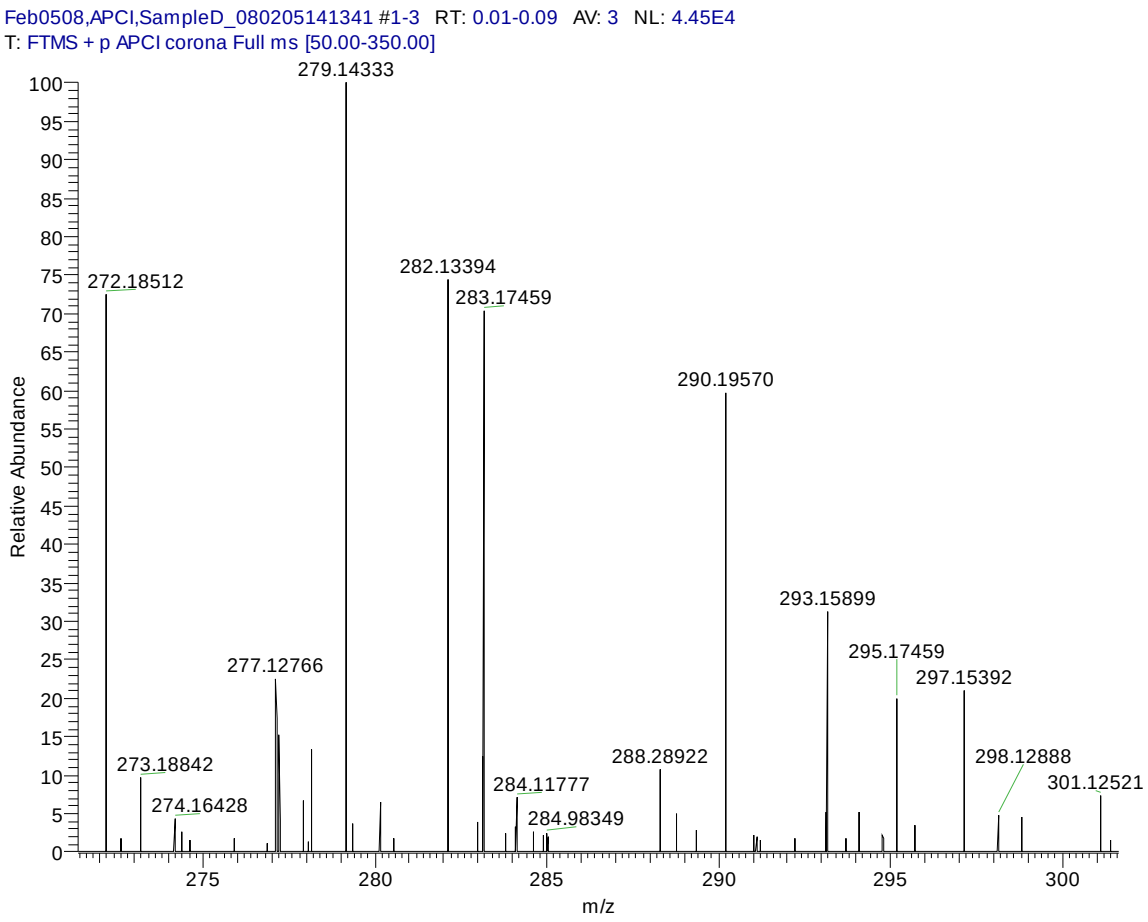

Figure 28. Mass Spectrum of the product of the reaction of PITC and 1-octanethiol. The sample was successfully ionized using atmospheric pressure chemical ionization (APCI) technique. The peak of interest has a mass to charge ratio of 282.13394.

Elemental composition search on mass 282.13394

m/z= 277.13394-287.13394

m/z	Theo. Mass	Delta (ppm)	RDB equiv.	Composition
282.13394	282.13447	-1.88	4.5	$C_{15}H_{24}N_{1}{}^{32}S_{2}$
	282.13179	7.62	0.0	$C_{12}H_{26}O_{3}{}^{32}S_{2}$
	282.13045	12.38	0.5	$C_{10}H_{24}O_{2}N_{3}{}^{32}S_{2}$
	282.12910	17.14	1.0	$C_{8}H_{22}O_{1}N_{6}{}^{32}S_{2}$

Figure 29. Elemental analysis of the peak of interest which has a mass to charge ratio of 282.13394.

II.B. Stability of Product

HPLC Data of the Stability of the Product of the Reaction of PITC and PEA at pH 7.4

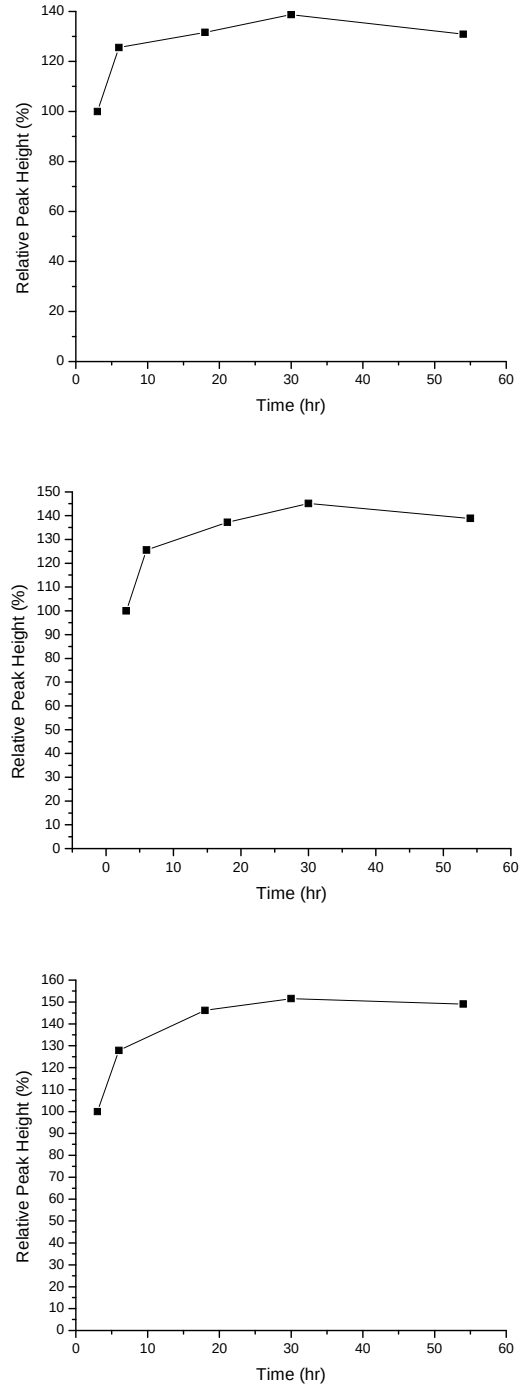

Figure 30. Three data sets of the time course of the stability of the product of the reaction of PITC and PEA at pH 7.4

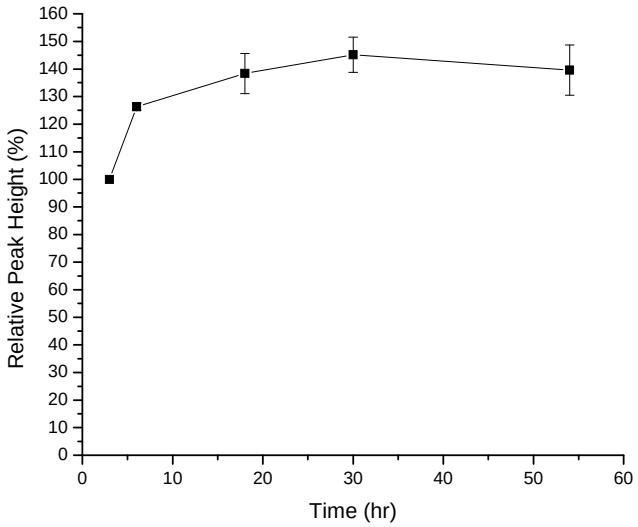

Figure 31. Time course (n=3) of the stability of the product of the reaction of PITC and PEA at pH 7.4

HPLC Data of the Stability of the Product of the Reaction of PITC and PEA at pH 9.0

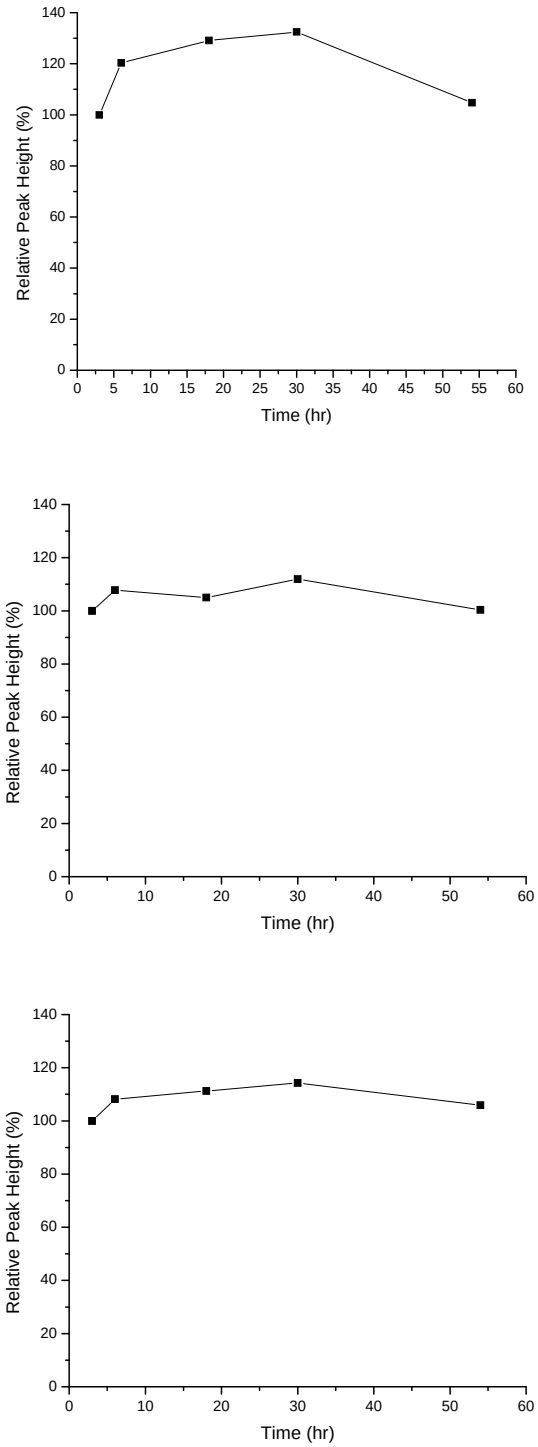

Figure 32. Three data sets of the time course of the stability of the product of the reaction of PITC and PEA at pH 9.0

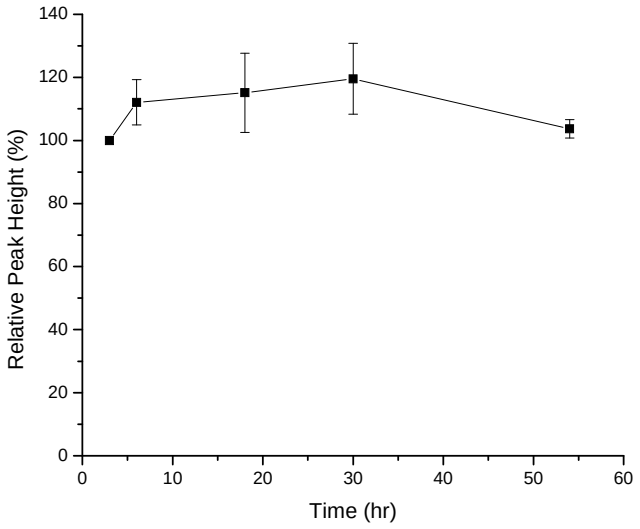

Figure 33. Time course (n=3) of the stability of the product of the reaction of PITC and PEA at pH 9.0

HPLC Data of the Stability of the Product of the Reaction of PITC and1-Octanethiol at pH 7.4

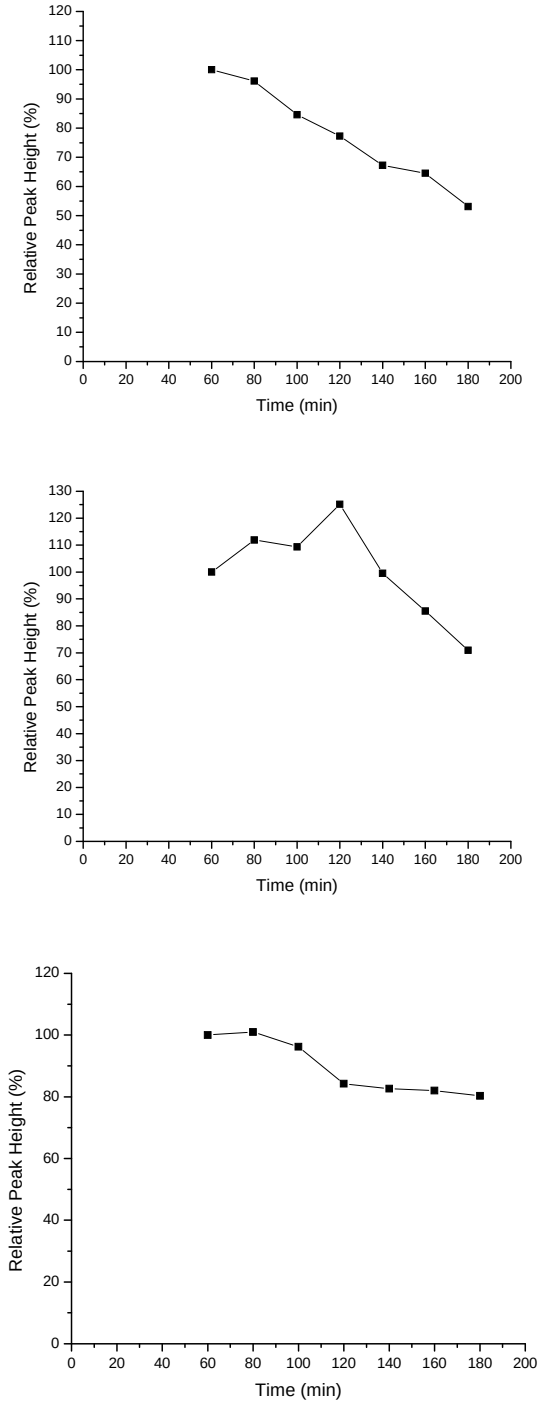

Figure 34. Three data sets of the time course of the stability of the product of the reaction of PITC and 1-octanethiol at pH 7.4

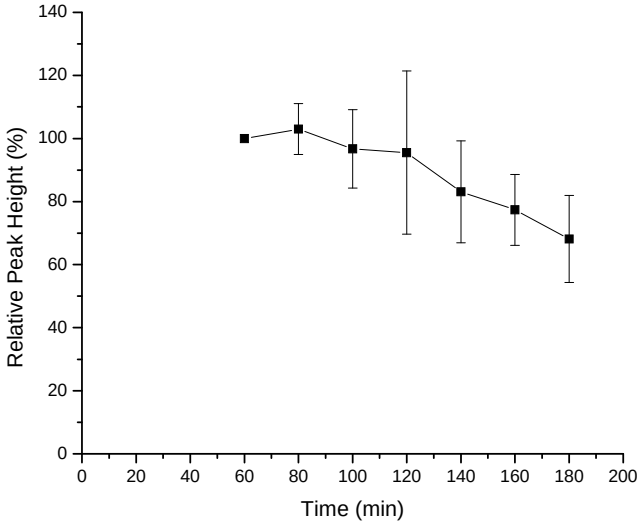

Figure 35. Time course (n=3) of the stability of the product of the reaction of PITC and 1-octanethiol at pH 7.4

HPLC Data of the Stability of the Product of the Reaction of PITC and 1-Octanethiol at pH 9.0

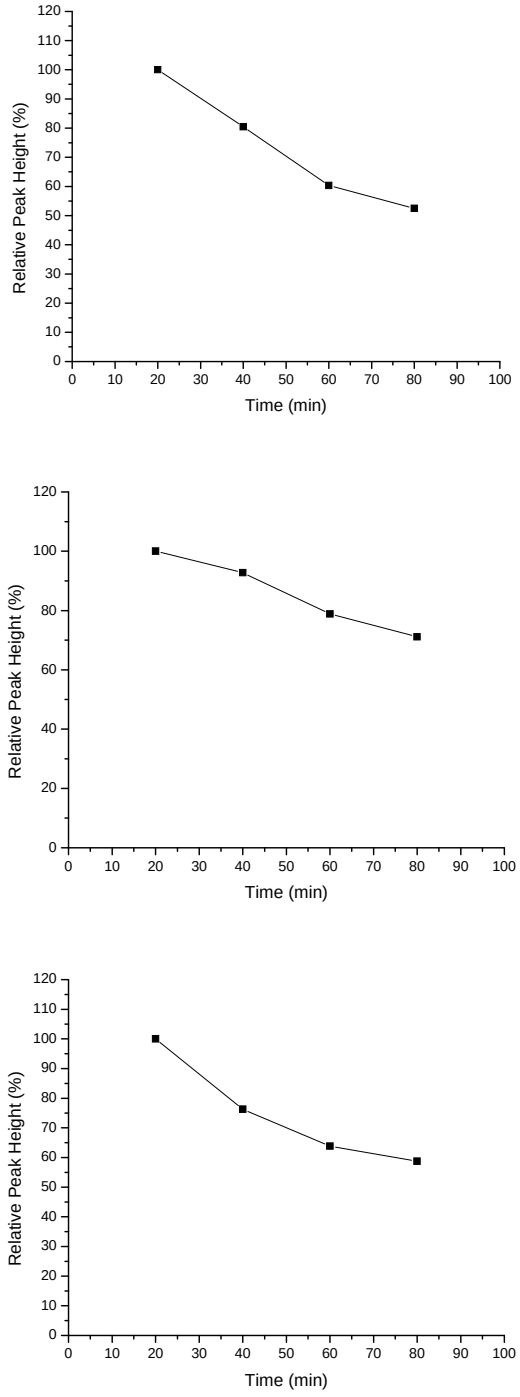

Figure 36. Three data sets of the time course of the stability of the product of the reaction of PITC and 1-octanethol at pH 9.0

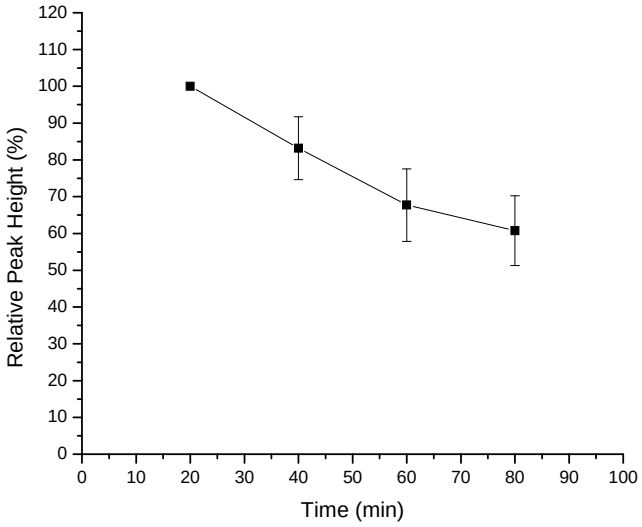

Figure 37. Time course (n=3) of the stability of the product of the reaction of PITC and 1-octanethoil at pH 9.0

RESULTS

I.A. HPLC Analysis of the Reaction of PITC with Amino Acid Analogs

Kinetic Analysis of the Background Degradation of PITC at pH 7.4

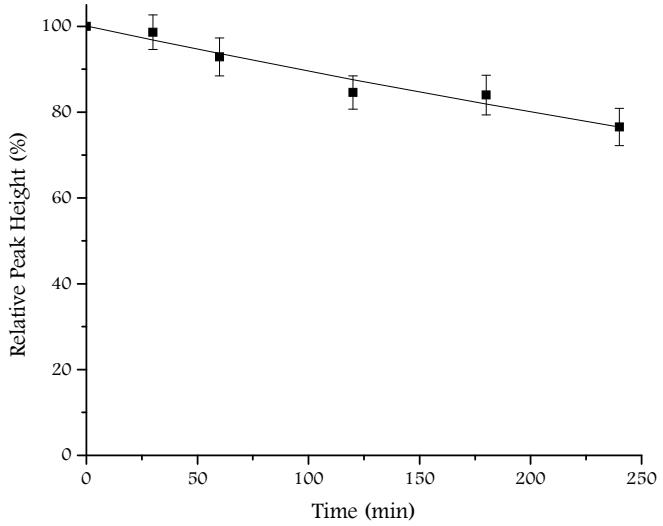

Figure 38. Analysis of the background degradation of PITC at pH 7.4 gave the following kinetic values;

$k = 0.00112 \pm 0.00012\ min^{-1}$

$y_0 = 100.1 \pm 1.4\ \%$

$R^2 = 0.960$

Kinetic Analysis of the Reaction of PITC with PEA at pH 7.4

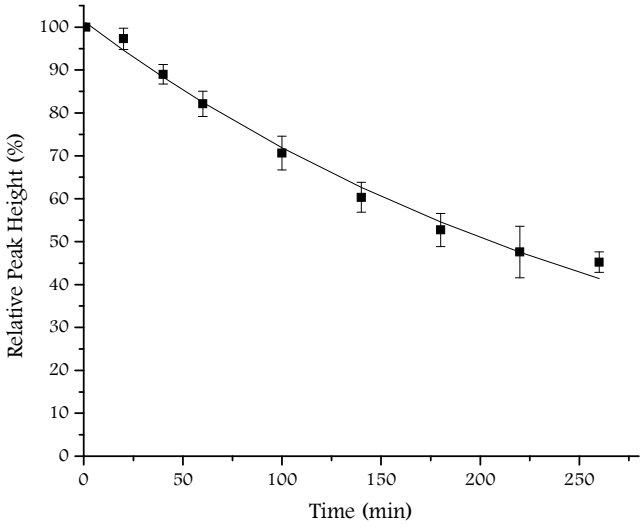

Figure 39. Analysis of the reaction of PITC with PEA at pH 7.4 gave the following kinetic values;

$k = 0.00344 \pm 0.00014\ min^{-1}$

$y_0 = 101.4 \pm 1.4\ \%$

$R^2 = 0.991$

Kinetic Analysis of the Reaction of PITC with 1-Octanethiol at pH 7.4

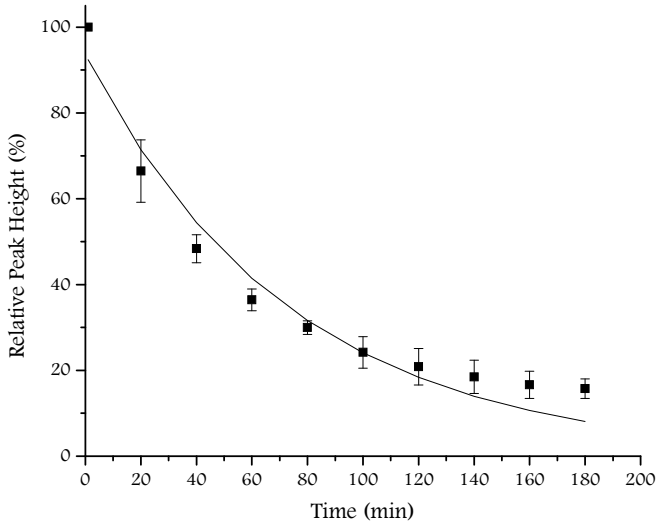

Figure 40. Analysis of the reaction of PITC with 1-octanethiol at pH 7.4 gave the following kinetic values;

$k = 0.0136 \pm 0.0012\ min^{-1}$

$y_0 = 93.7 \pm 4.9\ \%$

$R^2 = 0.960$

Fitting the data of the reaction of PITC with 1-octanethiol to a pseudo first order reaction did not give an accurate fit. There appears to be a slow process and a fast process in the reaction. A second fit of the data was done to the equation of the form;

$$y = y_0 * (e^{(-k1*t)} + e^{(-k2*t)})$$

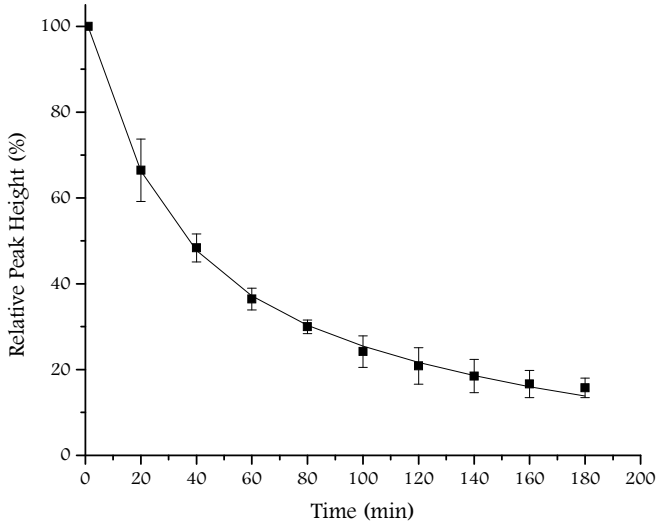

Figure 41. Analysis of the reaction of PITC with 1-octanethiol at pH 7.4 gave the following kinetic values;

$k1 = 0.00729 \pm 0.00019\ min^{-1}$

$k2 = 0.0422 \pm 0.00236\ min^{-1}$

$y_0 = 51.2 \pm 0.56\ \%$

$R^2 = 0.999$

Kinetic Analysis of the Reaction of PITC with Phenol at pH 7.4

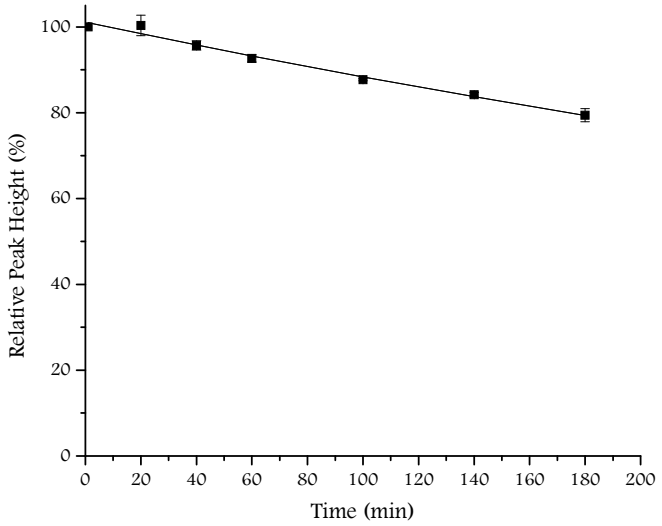

Figure 42. Analysis of the reaction of PITC with phenol at pH 7.4 gave the following kinetic values;

$k = 0.00135 \pm 0.00008\ min^{-1}$

$y_0 = 101.1 \pm 0.682\ \%$

$R^2 = 0.985$

Kinetic Analysis of the Background Degradation of PITC at pH 9.0

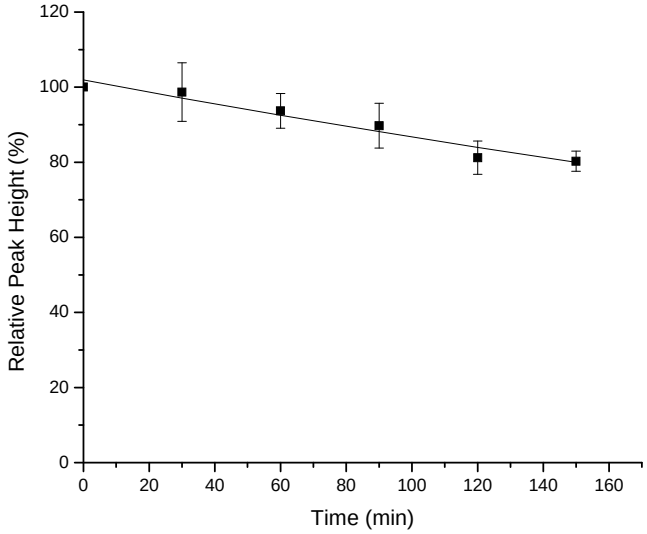

Figure 43. Analysis of the background degradation of PITC at pH 9.0 gave the following kinetic values;

$k = 0.00162 \pm 0.00019\ min^{-1}$

$y_0 = 101.9 \pm 1.60\ \%$

$R^2 = 0.95$

Kinetic Analysis of the Reaction of PITC with PEA at pH 9.0

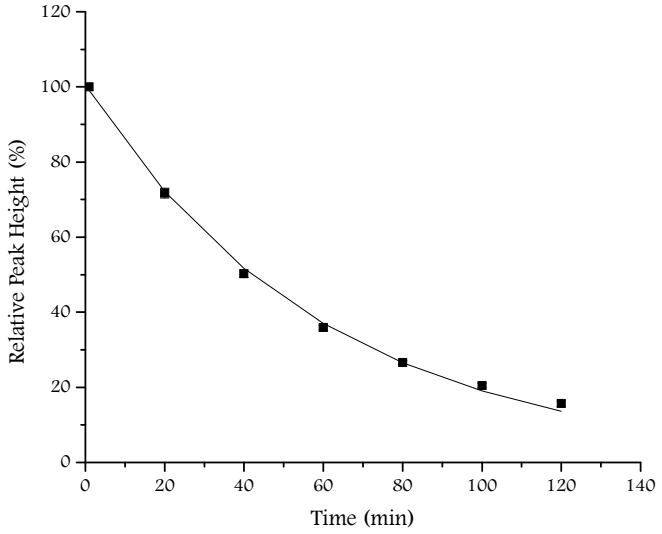

Figure 44. Analysis of the reaction of PITC with PEA at pH 9.0 gave the following kinetic values;

$k = 0.0167 \pm 0.0004\ min^{-1}$

$y_0 = 100.7 \pm 1.33\ \%$

$R^2 = 0.998$

Kinetic Analysis of the Reaction of PITC with 1-Octanethiol at pH 9.0

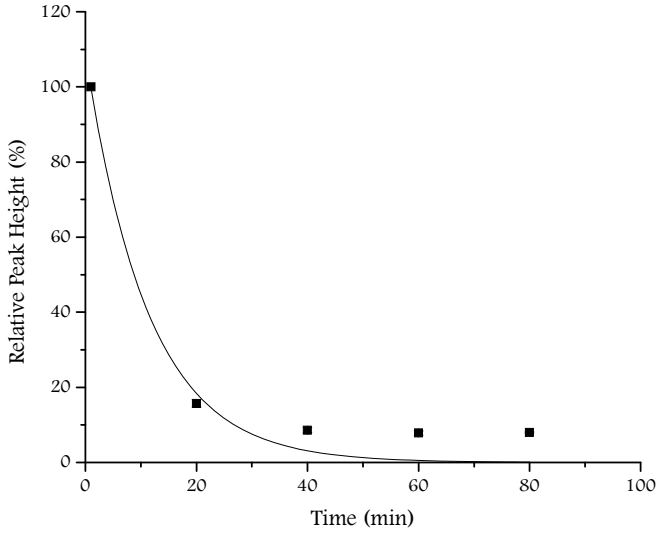

Figure 45. Analysis of the reaction of PITC with 1-octanethiol at pH 9.0 gave the following kinetic values;

$k = 0.0889 \pm 0.0196\ min^{-1}$

$y_0 = 109.0 \pm 8.46\ \%$

$R^2 = 0.977$

Fitting the data of the reaction of PITC with 1-octanethiol to a pseudo first order reaction did not give an accurate fit. There appears to be a slow process and a fast process in the reaction. A second fit of the data was done to the equation of the form;

$$y = y_0 * (e^{(-k1*t)} + e^{(-k2*t)})$$

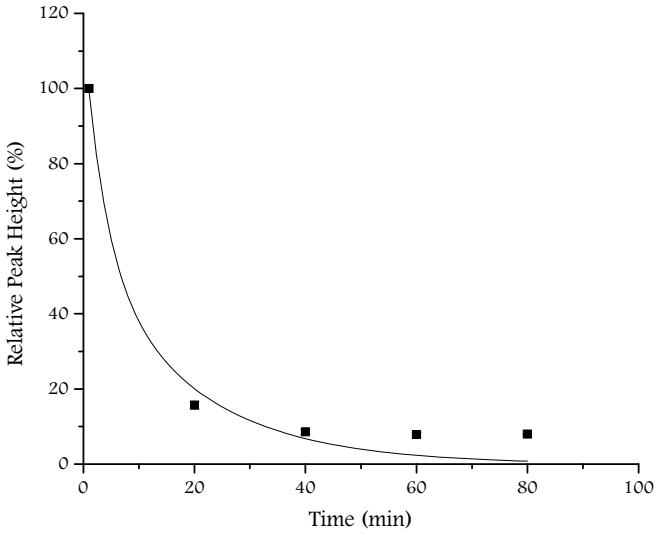

Figure 46. Analysis of the reaction of PITC with 1-octanethiol at pH 9.0 gave the following kinetic values;

$k1 = 0.00536 \pm 0.091\ min^{-1}$

$k2 = 0.264 \pm 9.99\ min^{-1}$

$y_0 = 57.9 \pm 261.9\ \%$

$R^2 = 0.984$

Kinetic Analysis of the Reaction of PITC with Phenol at pH 9.0

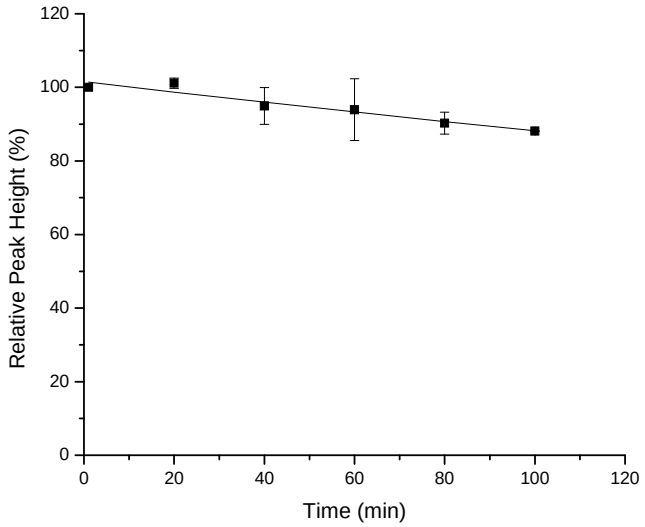

Figure 47. Analysis of the reaction of PITC with phenol at pH 9.0 gave the following kinetic values;

$k = 0.00141 \pm 0.0002\ min^{-1}$

$y_0 = 101.6 \pm 1.15\ \%$

$R^2 = 0.929$

Summary

Reaction	pH 7.4		pH 9.0	
	k (min^{-1})	Background Corrected k (min^{-1})	k (min^{-1})	Background Corrected k (min^{-1})
Background Degradation of PITC	1.12×10^{-3}	0	1.62×10^{-3}	0
PITC and PEA	3.44×10^{-3}	2.32×10^{-3}	1.67×10^{-2}	1.51×10^{-2}
PITC and 1-octanethiol	1.36×10^{-2}	1.26×10^{-2}	8.89×10^{-2}	8.73×10^{-2}
PITC and phenol	1.35×10^{-3}	2.3×10^{-4}	1.41×10^{-3}	-2.1×10^{-4} *

Table 2. Summary table of the pseudo first order rate constants of the reactions of PITC with amino acid analogs. Each rate constant was background corrected for the loss of PITC due to degradation.

* Although phenol has a negative rate constant at pH 9.0, the error generated from the fitting of the background degradation, which was $\pm$ 0.0002, is as large as the rate constant. Therefore the result is interpreted as a 0 rate constant.

II.A. High Resolution Mass Spectrometry Analysis of Products

Mass Spectrometry Analysis of the Product of the Reaction of PITC and PEA

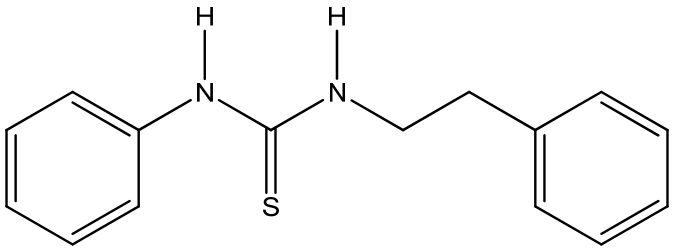

1-phenethyl-3-phenylthiourea

Figure 48. Structure of 1-phenethyl-3-phenylthiourea. The structure of this was confirmed by mass spectrometry analysis.

Mass Spectrometry Analysis of the Product of the Reaction of PITC and PEA

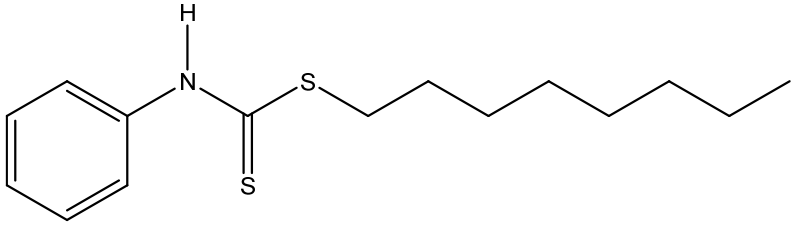

octyl phenylcarbamodithioate

Figure 49. Structure of octyl phenylcarbamodithioate. The structure of this was confirmed by mass spectrometry analysis.

DISCUSSION

This thesis investigated the kinetics of the chemical reaction between phenylisothiocyanate and amino acid analogs and the stability of their products. The information gained from these studies has given insight as to why isothiocyanate derivative cocaine analogs are difficult to use in hDAT labeling experiments. Comparing the rate constants of the reactions revealed that some amino acid analogs reacted more readily with isothiocyanate than others. In addition the products formed vary in stability.

Reactivity of Amino Acid Analogs at pH 7.4

A large excess of each amino acid analog was reacted with PITC in a solution at pH 7.4. The data obtained from these experiments were averaged and fitted to pseudo first order kinetic equations to get rate constants for the loss of PITC. All rate constants were background corrected by 1.12×10^{-3} min^{-1} to account for the degradation of PITC [Table 2]. The results showed that 1-octanethiol was the most reactive amino acid analog with a rate constant of $k = 1.26 \times 10^{-2}$ min^{-1}. The next most reactive analog was PEA with a rate constant of $k = 2.32 \times 10^{-3}$ min^{-1}. The least reactive amino acid analog was phenol which did not appear to react at all. There was a very small loss of PITC, but no detectable product was formed. The rate constant for the reaction of PITC and phenol was $k = 2.3 \times 10^{-4}$ min^{-1}. The error generated from the fitting of the background degradation of PITC was $\pm$ 0.0002. The statistical error in the calculation is as large as the rate constant, therefore the result is interpreted as no detectable reaction occurred between PITC and phenol.

These amino acid analogs are able to react with PITC because their functional groups have nucleophilic properties. The carbon atom in the isothiocyanate group (–NCS) is a good electrophile because it is surrounded by both nitrogen and sulfur which have a high electron affinity. These electron withdrawing groups pull electron density away from the carbon atom and give it a slight positive charge [Figure 52].

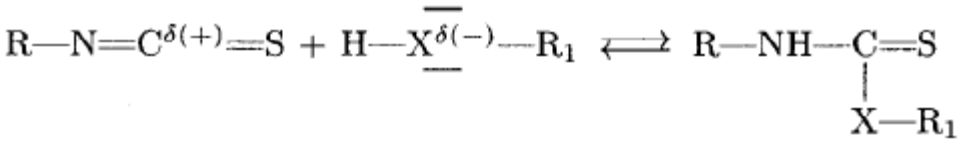

Figure 50. A schematic representation of the nucleophilic attack on the partially positive carbon of the isothiocyanate group by a partially positive nucleophile (Breier et al., 2000).

Reactivity of Amino Acid Analogs at pH 9.0

Repeating the experiments at pH 9.0 showed that pH does have an effect on reactivity. . All rate constants were background corrected by 1.62×10^{-3} min^{-1} to account for the degradation of PITC. 1-octanethiol remained the most reactive amino acid analog with a seven times faster rate constant of $k = 8.73 \times 10^{-2}$ min^{-1} at pH 9.0 than at pH 7.4. PEA also had a large change in reactivity with a six times faster rate constant of $k = 1.51 \times 10^{-2}$ min^{-1} at pH 9.0 than at pH 7.4. Strangely phenol had a background corrected rate constant of $k = -2.1 \times 10^{-4}$ min^{-1}. The error generated from the fitting of the background degradation of PITC was $\pm$ 0.0002. The statistical error in the calculation is as large as

the rate constant, therefore the result is interpreted as no detectable reaction occurred between PITC and phenol.

The increase in reactivity of these amino acid analogs observed at an increased pH can be analyzed by looking at their pKa values. 1-octanethiol has a pKa of 10.64, phenethylamine of 9.90 and phenol of 9.99. At pH 7.4, the percent of ionized species for –SH is ~0.06 %, for -NH_2 is 0.3 % and -OH is ~0.3 %. At pH 9.0, the percent of ionized species for –SH is 2.3 %, for -NH_2 is ~12.5 % and for -OH is ~10 %. There is 30-40 % increase in the concentration of ionized species for all the functional groups. The more ionized these functional groups are, the more nuclephilic they become and the better they are at attacking the electrophilic carbon of the isothiocyanate group (-NCS) [Figure x]. This increase in the amount of ionized species at pH 9.0, can account for the increase in the rate constants of 1-octanethiol and PEA from pH 7.4 to pH 9.0. A study of MFZ 3-37 labeling showed that there was more specific and more non-specific labeling of hDAT at pH 9.0 (Wirtz, 2004). Increasing the pH of the labeling experiment increased the reactivity of the nucleophilic amino acids in hDAT and could have caused the increase in labeling.

Identity and Stability of Products

The product of the reaction of PITC and the primary amine group of PEA was determined using high resolution mass spectrometry. The product is 1-phenethyl-3-phenylthiourea [Figure 48]. This compound appears to be very stable at both pH 7.4 and pH 9.0. In fact results show no detectable degradation for over 48 hours. The product of the reaction between PITC and the thiol group of 1-octanethiol is octyl phenylcarbamodithioate [Figure 49]. This compound appears to be highly unstable. At pH 7.4, the compound starts to show detectable degradation at 60 minutes and at pH 9.0 it starts to show degradation as early as 20 minutes into the reaction.

The stability of these products is representative of the stability of the bonds between isothiocyanate and amino acid residues in hDAT labeling. If a lysine residue is being labeled, the ligand should be able to stay attached to the protein during proteolysis and other processes. If it is cysteine that is being labeled, the ligand may dissociate from the protein during proteolytic processes and could lead to a low yield or no yield of labeled peptide. One of the reasons isothiocyanate derivative cocaine analogs were developed for use in labeling experiments was because they had a high yield. It was expected that there would be enough isothiocyanate labeled hDAT peptides to get a large enough sample for detection by mass spectrometertry. The information obtained from these stability tests show that, if a cysteine is being labeled, dissociation of the ligand from its peptide can lead to low yields and therefore poor detectability by mass spectrometry.

Summary

The results detailed in this thesis show that isothiocyanate derivative cocaine analogs may not be suitable for irreversible hDAT labeling experiments involving complex sample work ups, including gel electrophoresis, enzymatic digestion and further purification by HPLC and other methods. Although the isothiocyanate reacts well with lysine and cysteine residues, the bond created may not be stable. The bond between isothiocyanate and thiol groups dissociates quickly. If the isothiocyanate derivative cocaine analog labels a cysteine, it may detach from the protein during proteolytic processes. The loss of the label during proteolysis leads to a low yield of labeled peptide and there may not be enough sample for detection by high resolution mass spectrometry.

REFERENCES

Appell, M., Berfield, J.L., Wang, L.C., Dunn III, W.J., Chen, N.H., and Reith, M.E.A. (2004) Structure-activity relationships for substrate recognition by the human dopamine transporter. *Biochem. Pharmacol*.,**67**, 293-302.

Abramson, J., Smirnova, I., Kasho, V., Verner, G., Iwata, S., and Kaback, H.R. (2003) The lactose permease of Escherichia coli: overall structure, the sugar-binding site and the altering access model for transport. *FEBS Letters*, **555**, 96-101.

Berman, S.B., Zigmond, M.J., and Hastings, T.G. (1996) Modification of dopamine transporter function: effect of reactive oxygen species and dopamine. *J. Neurochem*., **67**, 593-600.

Berfield, J.L., Wang, L.C., and Reith, M.E.A. (1998) Which form of dopamine is the substrate for the human dopamine transporter: the cationic or the uncharged species. *J. Biol. Chem*., **274**, 4876-4882.

Carroll, F. I., Howell, L.L., and Kuhar, M.J. (1999) Pharmacotherapies for treatment of cocaine abuse: preclinical aspects. *J. Med. Chem*., **42**, 2721-2736.

Carroll, F. I., Lewin, A.H., Boja, J. W., and Kuhar, M.J. (1992) Cocaine receptor: biochemical characterization and structure-activity relationships of cocaine analogues at the dopamine transporter. *J. Med. Chem*., **35**, 969-981.

Carroll, F. I., Lewin, A.H., and Mascarella, S.W. (2002) Dopamine transporter uptake blockers structure-activity relationship. *In Neurotransmitter Transporters: Structure, Function, and Regulation*. Ed. M.E.A. Reith., Humana Press Inc., Totowa, NJ, 381-423.

Chen, N., and Justice, J.B. (2000) Differential effect of structural modification of human dopamine transporter on the inward and outward transport of dopamine. *Mol.Brain Res*., **75**, 208-215.

Chen, N., and Justice, J.B. (1998) Cocaine acts as an apparent competitive inhibitor at the outward facing conformation of the human norepinephrine transporter: kinetic analysis of inward and outward transport. *J. Neurochem*., **18**, 10257-10268.

Chen, N., Trowbridge, C.G., and Justice, J.B. (1998) Voltametric studies on mechanisms of dopamine efflux in the presence of substrates and cocaine from cells expressing human norepinephrine transporter. *J. Neurochem*., **71**, 653-665.

Chen, N. and Reith, M.E.A. (2000) Structure and function of the dopamine transporter. *Eur. J. Pharm*., **405**, 329-339.

Dorman, G., and Prestwich, G.D. (2000) Using photolabile ligands in drug discovery and development. *Trends Biotechnol.*, **18**, 64-77.

Edvardsen, O. and Dahl, S.G. (1994) A Putative Model of the Dopamine Transporter. *Molecular Brain Research*, **27**, 265-274.

Eshleman, A.J., Neve, R.L., Janowsky, A., and Neve, K.A. (1995) Characterization of a recombinant human dopamine transporter in multiple cell lines. *J. Pharm.Exp.Ther.*, **274**, 276-283.

Eshleman, A.J., Henningsen, R.A., Neve, K.A., and Janowsky, A. (1993) Release of dopamine via the human transporter. *Mol. Pharmacol*., **45**, 312-316.

Ferrer, J.V., Javitch, J.A. (1998) Cocaine Alters the Accessibility of Endogenous Cysteines in Putative Extracellular and Intracellular Loops of the Human Dopamine Transporter. *Proc. Natl. Acad. Sci. USA*, **95,** 9238-9243

Fiorino, D.F., Coury, A., Fibiger, H.C., and Phillips, A.G. (1993) Electrical stimulation of reward sites in the ventral tegmental area increases dopamine transmission in the nucleus accumbens of the rat. *Behav. Brain Res.*, **55**, 131-141.

Giros, B. and Caron, M. (1993) Molecular characterization of the dopamine transporter. *Trends Pharmacol. Sci.,* **14**, 43-39.

Giros, B., Mestikawy, S.E., Godinot, N., Zheng, K., Han, H., Yang-Feng, T., and Caron, M.G. (1992) Cloning, pharmacological characterization, and chromosome assignment of the human dopamine transporter. *Mol. Pharm.*, **42**, 383-390.

Gu, H., Wall, S.C., and Rudnick, G. (1993) Stable expression of biogenic amine transporters reveals differences in inhibitor sensitivity, kinetics, and ion dependence. *J. Biol. Chem.*, **269,** 7124-7130.

Hastrup, H., Sen, N., and Javitch, J.A. (2003) The human dopamine transporter forms a tetramer in the plasma membrane. *J. Biol. Chem.*, **278,** 45045-45048.

Indarte, M., Madura, J.D., Surratt C.K. (2008) Dopamine Transporter Comparative Molecular Modeling and Binding Site Prediction Using the $LeuT_{Aa}$ Leucine Transporter as a Template. *Proteins*, **70**, 1033-1046.

Johnson, R.A., Eshleman, A.J., Meyers, T., Neve, K.A., Janowsky, A. (1998) [3H] substrate and cell specific effects of uptake inhibitors on human dopamine and serotonin transporter mediated efflux. *Synapse*, **30**, 97-106.

Kahlig, K.M. and Galli, A. (2003) Regulation of dopamine transporter function and plasma membrane expression by dopamine, amphetamine, and cocaine. *Eur. J. Pharm.*, **479**, 153-158.

Kitayama, S., Shimanda, S., Xu, H., Markham, L., Donovan, D.M., and Uhl, G.R. (1992) Dopamine transporter site-directed mutations differentially alter substrate transport and cocaine binding. *Proc. Natl. Acad. Sci. USA*, **89**, 7782-7785.

Kotzyba-Hibert, F., Kapfer, I., and Goeldner, M. (1995) Recent trends in photoaffinity labeling. *Angew.Chem. Int. Ed. Engl*., **34**, 1296-1312.

Kuhar, M.J., Ritz, M.C., and Boja, J.W. (1991) The dopamine hypothesis of the reinforcing properties of cocaine. *Trends in Neuroscience*, **14**, 299-302.

Lever T.M., Codgell R.J., Lindsay J.G. (1994) Analysis of Membrane Proteins: Current Problems and Future Perspectives. *In Membrane Expression Systems. A User's Guide.* G.W. Gould (ed.) Portland Press, London.

Lever, J.R., Zou, M.F., Parnas, L.M., Duval, R.A., Wirtz, S.E., Justice, J.B., Vaughan, R.A., Newman, A.H. (2004) Radioiodinated Azide and Isothiocyanate Derivatives of Cocaine for Irreversible of Dopamine Transporter; Synthesis and Covalent Binding Studies. *Bioconjugate Chem*, **16**, 644-649.

Lin, Z., Itokawa, M., and Uhl, G.R. (2000) Dopamine transporter praline mutations influence dopamine uptake, cocaine analog recognition, and expression. *Faseb, J*., **14**, 715-728.

Norregaard, L., Visiers, I., Loland, C.J., Ballesteros, J., Weinstein, H., and Gether, U. (2002) Structural probing of a microdomain in the dopamine transporter. *Biochemistry*, **39**, 15836-15846.

New Science Press (2002) Membrane protein structure: the principle governing the structures of integral membrane proteins are the same as those for water-soluble proteins and lead to formation of the same secondary structure elements.

McElvain, J. S. and Schenk J.O. (1992) A multisubstrate mechanism of striatal dopamine uptake and its inhibition by cocaine. *J. Neurochem.*, **43,** 2189-2199.

Meiergerd, S.M., and Schenk, J.O. (1994) Striatral transporter for dopamine: catechol structure-activity studies and susceptibility to chemical modification. *J. Neurochem.*, **62,** 998-1008.

Ravna, A.W., Sylte, I., and Dahl, S.G. (2003) Molecular model of the neural dopamine transporter. *J. Comput- Aided Mate. Des.*, **17**, 367-382.

Reed, B. (2001) Photaffinity labeling and peptide mapping of the human dopamine transporter. *PhD thesis defense*, Emory University.

Reith, M.E.A., Xu, C., Zhang, L., and Coffey, L.L. (1996) Translocation of dopamine and binding of WIN 35,428 measured under identical conditions in cells expressing the cloned human dopamine transporter. *Naunyn Schmiedeberg's Arch Pharmacol.*, **345**, 295-304.

Reith, M.E.A., Bertfield, J.L., Zhang, L.C., Ferrer, J.V., and Javitch, J.A. (2001) The uptake inhibitors cocaine and benztropine differentially alter the conformation of the human dopamine transporter. *J. Biol. Chem.*, **276**, 29012-29018.

Rothman, R.B., Becketts, K.M., Radesca, L.R., de Costa, B.R., Rice, K.C., Carroll, F.I., and Dersch, C.M. (1993) Studies of the biogenic amine transporters. II. A brief study on the use of [^{3}H] DA-uptake-inhibition to transporter-binding-inhibition ratios for the in vitro evaluation of putative cocaine antagonists. *Life Sci.*, **53**, 267-272.

Ritz, M.C., Lamb, R.J., Goldberg, S.R., and Kuhar, M. J. (1987) Cocaine receptors on dopamine transporters are related to self-administration of cocaine. *Science*, **237**, 1219-1223.

Rudnick, G. (2002) Mechanisms of biogenic amine neurotransmitter transporters. In *Neurotransmitter Transporters: Structure, Function, and Regulation*. Ed. M.E.A. Reith., Humana Press Inc., Totowa, NJ, 25-52.

Sallee, F.R., Fogel, E.L., Schwarz, E., Choi, S.M., Curran, D.P., and Niznik, H.B. (1989) Photoaffinity labeling of the mammalian dopamine transporter. *Fed. Euro. Biochem. Soc*., **256**, 219-224.

Satchell, D.P., Satchell, R.S. (1990) The Kinetics and Mechanism of Aminolysis of Isothiocyanates. *J. Chem. Soc*., 1415-1419.

Torres, G.E., Carneiro, A., Seamans, K., Fiorentini, C., Sweeney, A., Yao, W.D., and Caron, M.G. (2003) Oligomerization and trafficking of the human dopamine transporter. *J. Biol. Chem*., **278**, 2731-2739.

Uhl G.R., Lin Z. (2003) The Top 20 Dopamine Transporter Mutants: Structure-Function Relationships and Cocaine Addictions. *Eur. J. Pharmacol.*, **479**, 71-82.

Vandenbergh D.J., Persico A.M., Hawkins A.L., Griffin C.A., Li X., Jabs E.W., Uhl G.R. (1992) Human Dopamine Transporter Gene (DAT1) Maps to Chromosome 5p15.3 and Displays a VNTR. *Genomics*, **14**, 1104-1006.

Vaughan R.A., Uhl G. Kuhar M.J. (1993) Recognition of Dopamine Transporters by Antipeptide Antibodies. *Mol. Cell. Neurosci.*, **4**, 209-215.

Vaughan, R.A., and Kuhar, M.J. (1996) Dopamine transporter ligand binding domain. *J. Biol.Chem.*, **271**, 21672-21680.

Vaughan, R.A., Agoston, G.E., Lever, J.R., and Newman, A.H. (1999) Differential binding of tropane-based photoaffinity ligands on the dopamine transporter. *J.Neurosci.*, **19**, 630-636.

Vaughan, R.A. (1995) Photoaffinity-labeled ligand binding domains on dopamine transporters identified by peptide mapping. *Mol. Phar*., **47**, 956-964.

Vaughan R.A., Gaffaney J.D., Lever J.R., Reith M.E.A., Dutta A.K. (2001) Dual Incoporation of Photoaffinity Ligands on Dopamine Transporters implicates Proximity of Labeled Domains. *Mol. Pharmacol.*, **59(5)**, 1157-1164.

Vaughan R.A., Parnas M.L., Gaffaney J.D., Lowe M.J., Wirtz S., Pham A., Reed B., Dutta S.M., Murray K.K., Justice J.B. (2005) Affinity Labeling the Dopamine Transporter Ligand Binding Site. *J. Neurosci. Methods*, 143(1), 33-40.

Volz, T.H., Schenk, J.O. (2005) A Comprehensive Atlas of the Topography of Functional Groups of the Dopamine Transporter. *Synapse*, **58**, 72-94.

Wirtz S. (2004) Identification of an MFZ 2-24 Affinity Labeling Site on the Human Dopamine Transporter. PhD Dissertation, Emory Univerysity.

Wu X., Gu H.H. (2003) Cocaine Affinity Decreased by Mutations of Aromatic Residue Phenylalanine 105 in the Transmembrane Domain 2 of Dopamine Transporter. *Mol. Pharmacol.*, **63**, 653-658.

Xu, C., Coffey, L.L., and Reith, M.E.A. (1997) Binding domains for blockers and substrates on the dopamine transporter in rat striatal membranes studied by protection against N-ethylmaleimide-induced reduction of [^{3}H] Win 35,428 binding**.** *Naunyn Schmiedeberg's Arch Pharmacol.*, **355**, 64-73.

Yamashita, A., Singh, S.K., Kawate, T., Jin, Y., Gouaux, E. (2005) Crystal Structure of a Bacterial Homologue of Na+/Cl- Dependent Neurotransmitter Transporters. *Nature,* **437**, 215-223.

Zou, M.F., Kopajtic, T., Katz, J., Wirtz, S.E., Justice, J.B., Newman, A.H. (2001) Novel Tropane-Based Irreversible Ligands for the Dopamine Transporter. *J. Med. Chem.*, **44**, 4453-4461.